(12) INTERNATIONAL APPLICATION PUBLISHED UNDER THE PATENT COOPERATION TREATY (PCT)

(19) World Intellectual Property Organization
International Bureau

(43) International Publication Date
11 September 2015 (11.09.2015)

WIPO | PCT

(10) International Publication Number
WO 2015/134740 A1

(51) International Patent Classification:
G02B 27/22 (2006.01) *G02B 27/01* (2006.01)

(21) International Application Number:
PCT/US2015/018951

(22) International Filing Date:
5 March 2015 (05.03.2015)

(25) Filing Language: English

(26) Publication Language: English

(30) Priority Data:
61/948,226 5 March 2014 (05.03.2014) US

(71) Applicants: **ARIZONA BOARD OF REGENTS ON BEHALF OF THE UNIVERSITY OF ARIZONA** [US/US]; 220 West Sixth Street, 4th Floor, Tucson, AZ 85701 (US). **UNIVERSITY OF CONNECTICUT** [US/US]; Office Of The Vice President For Research, 400 Farmington Avenue - MC 6400, Farmington, CT 06032 (US).

(72) Inventors: **HUA, Hong**; College Of Optical Sciences, 1630 E. University Blvd., Tucson, AZ 85721 (US). **JAVIDI, Bahram**; University Of Connecticut, Electrical & Computer Engineering Dept., 371 Fairfield Road, Unit 4157, Storrs, CT 06269-4157 (US).

(74) Agents: **HAUN, Niels** et al.; Dann, Dorfman, Herrell And Skillman, P.C., 1601 Market Street, Suite 2400, Philadelphia, PA 19103-2037 (US).

(81) Designated States *(unless otherwise indicated, for every kind of national protection available)*: AE, AG, AL, AM, AO, AT, AU, AZ, BA, BB, BG, BH, BN, BR, BW, BY, BZ, CA, CH, CL, CN, CO, CR, CU, CZ, DE, DK, DM, DO, DZ, EC, EE, EG, ES, FI, GB, GD, GE, GH, GM, GT, HN, HR, HU, ID, IL, IN, IR, IS, JP, KE, KG, KN, KP, KR, KZ, LA, LC, LK, LR, LS, LU, LY, MA, MD, ME, MG, MK, MN, MW, MX, MY, MZ, NA, NG, NI, NO, NZ, OM, PA, PE, PG, PH, PL, PT, QA, RO, RS, RU, RW, SA, SC, SD, SE, SG, SK, SL, SM, ST, SV, SY, TH, TJ, TM, TN, TR, TT, TZ, UA, UG, US, UZ, VC, VN, ZA, ZM, ZW.

(84) Designated States *(unless otherwise indicated, for every kind of regional protection available)*: ARIPO (BW, GH, GM, KE, LR, LS, MW, MZ, NA, RW, SD, SL, ST, SZ, TZ, UG, ZM, ZW), Eurasian (AM, AZ, BY, KG, KZ, RU, TJ, TM), European (AL, AT, BE, BG, CH, CY, CZ, DE, DK, EE, ES, FI, FR, GB, GR, HR, HU, IE, IS, IT, LT, LU, LV, MC, MK, MT, NL, NO, PL, PT, RO, RS, SE, SI, SK, SM, TR), OAPI (BF, BJ, CF, CG, CI, CM, GA, GN, GQ, GW, KM, ML, MR, NE, SN, TD, TG).

Published:

— *with international search report (Art. 21(3))*

(54) Title: WEARABLE 3D AUGMENTED REALITY DISPLAY WITH VARIABLE FOCUS AND/OR OBJECT RECOGNITION

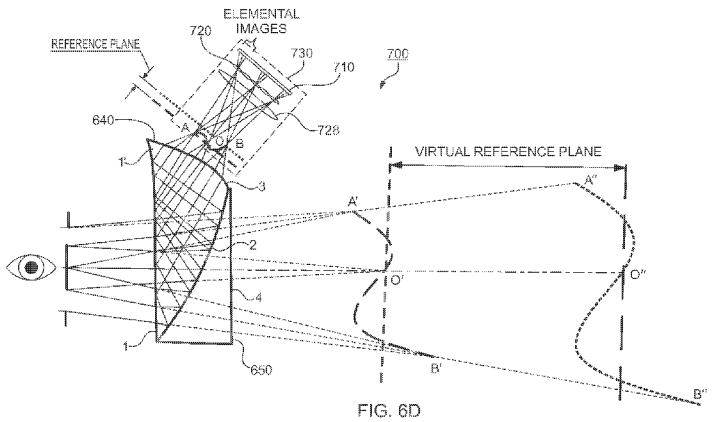

FIG. 6D

(57) Abstract: A wearable 3D augmented reality display and method, which may include 3D integral imaging optics.

WO 2015/134740 A1

WEARABLE 3D AUGMENTED REALITY DISPLAY WITH VARIABLE FOCUS AND/OR OBJECT RECOGNITION

Related Applications

[0001] This application of claims the benefit of priority of U.S. Provisional Application No.61/948,226, filed on March 5, 2014, the entire contents of which application(s) are incorporated herein by reference.

Government License Rights

[0002] This invention was made with government support under Grant Nos. 14-22653 and 14-22179 awarded by the National Science Foundation. The government has certain rights in the invention.

Field of the Invention

[0003] The present invention relates generally to a wearable 3D augmented reality display, and more particularly, but not exclusively, to a wearable 3D augmented reality display comprising 3D integral imaging (InI) optics with optional variable focus and/or object recognition.

Background of the Invention

[0004] An augmented reality (AR) display, which allows overlaying 2D or 3D digital information on a person's real-world view, has long been portrayed as a transformative technology to redefine the way we perceive and interact with digital information. Although several types of AR display devices have been explored, a desired form of AR displays is a lightweight optical see-through head-mounted display (OST-HMD), which enables optical superposition of digital information onto the direct view of the physical world and maintains see-through vision to the real world. With the rapidly increased bandwidth of wireless networks, the miniaturization of electronics, and the prevailing cloud computing, one of the current challenges is to realize an unobtrusive AR display that integrates the functions of OST-HMDs, smart phones, and mobile computing within the volume of a pair of eyeglasses.

[0005] Such an AR display, if available, will have the potential to revolutionize many fields of practice and penetrate through the fabric of life, including medical, defense and security, manufacturing, transportation, education and entertainment fields. For example, in medicine

AR technology may enable a physician to see CT images of a patient superimposed onto the patient's abdomen while performing surgery; in mobile computing it can allow a tourist to access reviews of restaurants in his or her sight while walking on the street; in military training it can allow fighters to be effectively trained in environments that blend 3D virtual objects into live training environments.

[0006] Typically, the most critical barriers of AR technology are defined by the displays. The lack of high-performance, compact and low-cost AR displays limits the ability to explore the full range of benefits potentially offered by AR technology. In recent years a significant research and market drive has been toward overcoming the cumbersome, helmet-like form factor of OST-HMD systems, primarily focusing on achieving compact and lightweight form factors. Several optical technologies have been explored, resulting in significant advances in OST-HMDs. For instance, the well-advertised Google Glass® is a very compact, lightweight (~36grams), monocular OST-HMD, providing the benefits of encumbrance-free instant access to digital information. Although it has demonstrated a promising and exciting future prospect of AR displays, the current version of Google Glass® has a very narrow FOV (approximately 15° FOV diagonally) with an image resolution of 640x360 pixels. It offers limited ability to effectively augment the real-world view in many applications.

[0007] Despite such promises a number of problems remain with existing OST-HMD's, such as visual discomfort of AR displays. Thus, it would be an advance in the art to provide OST-HMD's which provide increased visual comfort, while achieving low-cost, high-performance, lightweight, and true 3D OST-HMD systems.

Summary of the Invention

[0008] In one of its aspects the present invention may provide a 3D augmented reality display having a microdisplay for providing a virtual 3D image for display to a user. For example, the optical approach of the present invention may uniquely combine the optical paths of an AR display system with that of a micro-InI subsystem to provide a 3D lightfield optical source. This approach offers the potential to achieve an AR display invulnerable to the accommodation-convergence discrepancy problem. Benefiting from freeform optical technology, the approach can also create a lightweight and compact OST-HMD solution.

[0009] In this regard, in one exemplary configuration of the present invention, display optics may be provided to receive optical radiation from the microdisplay and may be configured to create a 3D lightfield, that is, a true optically reconstructed 3D real or virtual object from the received radiation. (As used herein the term "3D lightfield" is defined to mean the radiation

field of a 3D scene comprising a collection of light rays appearing to be emitted by the 3D scene to create the perception of a 3D scene.) An eyepiece in optical communication with the display optics may also be included, with the eyepiece configured to receive the 3D lightfield from the display optics and deliver the received radiation to an exit pupil of the system to provide a virtual display path. The eyepiece may include a selected surface configured to receive the 3D lightfield from the display optics and reflect the received radiation to an exit pupil of the system to provide a virtual display path. The selected surface may also be configured to receive optical radiation from a source other than the microdisplay and to transmit such optical radiation to the exit pupil to provide a see-through optical path. The eyepiece may include a freeform prism shape. In one exemplary configuration the display optics may include integral imaging optics.

Brief Description of the Drawings

[0010] The foregoing summary and the following detailed description of the exemplary embodiments of the present invention may be further understood when read in conjunction with the appended drawings, in which:

[0011] Figures 1A to 1C schematically illustrate accommodation-convergence cues in a monocular AR display (Fig. 1A); a binocular display (Fig. 1B); and, viewing a real object (Fig. 1C);

[0012] Figure 2 schematically illustrates a block diagram of an exemplary 3D-OST-HMD system in accordance with the present invention, comprising a microscopic integral imaging (InI) unit, see-through optics, and eyepiece;

[0013] Figure 3 schematically illustrates a diagram of a microscopic InI unit for creating a 3D lightfield of a 3D scene for use in devices and methods of the present invention;

[0014] Figure 4 schematically illustrates a diagram of an alternative exemplary microscopic InI (micro-InI) unit in accordance with the present invention for creating a 3D lightfield of a 3D scene where the virtual lightfield is telecentric;

[0015] Figure 5 schematically illustrates a diagram of an exemplary head-worn 3D integral imaging display system in accordance with the present invention, which integrates a micro-InI unit and conventional eyepiece optics for creating a virtual lightfield of a 3D scene;

[0016] Figures 6A to 6C schematically illustrate an exemplary design of a 3D augmented reality optical see-through HMD in accordance with the present invention using freeform optical technology, in which Fig. 6A illustrates an exemplary freeform eyepiece for 3D lightfield display, Fig. 6B illustrates an exemplary freeform corrector lens to correct viewing

axis deviations and aberrations, and Fig. 6C illustrates an integrated optical layout and raytracing;

[0017] Figure 6D schematically illustrates an exemplary design of a 3D augmented reality optical see-through HMD in accordance with the present invention including a vari-focal element;

[0018] Figure 6E schematically illustrates an exemplary design of a 3D augmented optical see-through HMD in accordance with the present invention including 3D and/or 2D object recognition;

[0019] Figure 7 schematically illustrates an exemplary micro-InI module and eyepiece in accordance with the present invention;

[0020] Figure 8 illustrates an exemplary prototype of a microdisplay, microlens array, 3D scene reconstructed by micro-InI, and a free form eyepiece in accordance with the present invention;

[0021] Figure 9 illustrates the experimental "3D" image used in a particular demonstration of the invention; and

[0022] Figures 10A to 10D demonstrate images captured by a digital camera placed at the eyepiece of the prototype of Fig. 8 where the camera was focused at 4 m (Fig. 10A), 30 cm (Fig. 10B), shifted to the left side of the exit pupil (Fig. 10C), and shifted to the right side of the exit pupil (Fig. 10D).

Detailed Description of the Invention

[0023] Despite current commercial development of HMDs, very limited efforts have been made to address the challenge of minimizing visual discomfort of AR displays, which is a critical concern in applications requiring an extended period of use. One of the key factors causing visual discomfort is the accommodation-convergence discrepancy between the displayed digital information and the real-world scene, which is a fundamental problem inherent to most of the existing AR displays. The accommodation cue refers to the focus action of the eye where ciliary muscles change the refractive power of the crystalline lens and therefore minimize the amount of blur for the fixated depth of the scene. Associated with eye accommodation change is the retinal image blur cue which refers to the image blurring effect varying with the distance from the eye's fixation point to the points nearer or further away. The accommodation and retinal image blurring effects together are known as focus cues. The convergence cue refers to the rotation action of the eyes to bring the visual axes inward or outward to intersect at a 3D object of interest at near or far distances.

[0024] The accommodation-convergence mismatch problem stems from the fact that the image source in most of the existing AR displays is a 2D flat surface located at a fixed distance from the eye. Consequently, this type of AR display lacks the ability to render correct focus cues for digital information that is to be overlaid over real objects located at distances other than the 2D image source. It causes the following three accommodation-convergence conflict. (1) There exists a mismatch of accommodation cues between the 2D image plane and the real-world scene (Fig. 1A). The eye is cued to accommodate at the 2D image plane for viewing the augmented information while the eye is concurrently cued to accommodate and converge at the depth of a real 3D object onto which the digital information is overlaid. The distance gap between the display plane and real-world objects can be easily beyond what the human visual system (HVS) can accommodate simultaneously. A simple example is the use of an AR display for driving assistance where the eyes need to constantly switch attention between the AR display and real-world objects spanning from near (e.g. dashboard) to far (e.g. road signs). (2) In a binocular stereoscopic display, by rendering a pair of stereoscopic images with binocular disparities, the augmented information may be rendered to appear at a different distance from the 2D display surface (Fig. 1B). When viewing augmented information, the eye is cued to accommodate at the 2D display surface to bring the virtual display in focus but at the same time the eye is forced to converge at the depth dictated by the binocular disparity to fuse the stereoscopic pair. In viewing a natural scene (Fig. 1C), the eye convergence depth coincides with the accommodation depth and objects at depths other than the object of interest are seen blurred. (3) Synthetic objects rendered via stereoscopic images, regardless of their rendered distance from the user, are seen all in focus if the viewer focuses on the image plane, or are seen all blurred if the user accommodates at distances other than the image plane. The retinal image blur of a displayed scene does not vary with the distances from an eye fixation point to other points at different depths in the simulated scene. In a nutshell, the incorrect focus cues may contribute to issues in viewing stereoscopic displays, such as distorted depth perception, diplopic vision, visual discomfort and fatigue, and degradation in oculomotor response.

[0025] In one of its aspects the present invention relates to a novel approach to OST-HMD designs by combining 3D lightfield creation technology and freeform optical technology. 3D lightfield creation technology of the present invention reconstructs the radiation field of a 3D scene by creating a collection of light rays appearing to be emitted by the 3D scene and creating the perception of a 3D scene. Thus, as used herein the term “3D lightfield” is

defined to mean the radiation field of a 3D scene comprising a collection of light rays appearing to be emitted by the 3D scene to create the perception of a 3D scene. The reconstructed 3D scene creates a 3D image source for HMD viewing optics, which enables the replacement of a typical 2D display surface with a 3D source and thus potentially overcomes the accommodation-convergence discrepancy problem. Any optical system capable of generating a 3D lightfield may be used in the devices and methods of the present invention. For instance, one exemplary configuration of the present invention uses micro integral imaging (micro-InI) optics for creating a full-parallax 3D lightfield to optically create the perception of the 3D scene. (Persons skilled in the art will be aware that Integral imaging (InI) is a multi-view imaging and display technique that captures or displays the light fields of a 3D scene by utilizing an array of pinholes, lenses or microlenses. In the case of being a display technique, a microlens array in combination with a display device, which provides a set of elemental images each having information of a different perspective of the 3D scene. The microlens array in combination with the display device renders ray bundles emitted by different pixels of the display device, and these ray bundles from different pixels intersect and optically create the perception of a 3D point that appears to emit light and occupy the 3D space. This method allows the reconstruction of a true 3D image of the 3D scene with full parallax information in all directions.) Other optical system capable of generating a 3D lightfield which may be used with the present invention include, but not limited to, holographic display (M. Lucente, "Interactive three-dimensional holographic displays: seeing the future in depth," Computer Graphics, 31(2), pp. 63-67, 1997; P.A. Blanche, et al, "Holographic three-dimensional telepresence using large-area photorefractive polymer", Nature, 468, 80-83, Nov. 2010), multi-layer computational lightfield display (G. Wetzstein et al., "Tensor Displays: Compressive light field synthesis using multilayer displays with directional backlighting," ACM Transactions on Graphics, 31(4), 2012.), and volumetric displays (Blundell, B. G., and Schwarz, A. J., "The classification of volumetric display systems: characteristics and predictability of the image space," IEEE Transaction on Visualization and Computer Graphics, 8(1), pp. 66-75, 2002. J. Y. Son, W.H. Son, S.K. Kim, K.H. Lee, B. Javidi, "Three-Dimensional Imaging for Creating Real-World-Like Environments," Proceedings of IEEE Journal, Vol. 101, issue 1, pp. 190-205, January 2013.).

[0026] A micro-InI system has the potential of achieving full-parallax 3D object reconstruction and visualization in a very compact form factor suitable for a wearable system. It can dramatically alleviate most of the limitations in a conventional autostereoscopic InI

display due to the benefit of well-constrained viewing positions and can be effectively utilized for addressing the accommodation-convergence discrepancy problem in conventional HMD systems. The micro-InI unit can reconstruct a miniature 3D scene through the intersection of propagated ray cones from a large number of recorded perspective images of a 3D scene. By taking advantage of the freeform optical technology, the approach of the present invention can result in a compact, lightweight, goggle-style AR display that is potentially less vulnerable to the accommodation-convergence discrepancy problem and visual fatigue. Responding to the accommodation-convergence discrepancy problem of existing AR displays, we developed an AR display technology with the ability to render the true lightfield of a 3D scene reconstructed optically and thus accurate focus cues for digital information placed across a large depth range.

[0027] The challenges of creating a lightweight and compact OST-HMD solution, invulnerable to the accommodation-convergence discrepancy problem, are to address two cornerstone issues. The first is to provide the capability of displaying a 3D scene with correctly rendered focus cues for a scene's intended distance correlated with the eye convergence depth in an AR display, rather than on a fixed-distance 2D plane. The second is to create an optical design of an eyepiece with a form factor as compelling as a pair of eyeglasses.

[0028] A block diagram of a 3D OST-HMD system in accordance with the present invention is illustrated in Fig. 2. It includes three principal subsystems: a lightfield creation module ("3D Lightfield Creation Module") reproducing the full-parallax lightfields of a 3D scene seen from constrained viewing zones; an eyepiece relaying the reconstructed 3D lightfields into a viewer's eye; and a see-through system ("See-through Optics") optically enabling a non-obtrusive view of the real world scene.

[0029] In one of its aspects, the present invention provides an innovative OST-HMD system that integrates the 3D micro-InI method for full-parallax 3D scene optical visualization with freeform optical technology for OST-HMD viewing optics. This approach enables the development of a compact 3D InI optical see-through HMD (InI-OST-HMD) with full-parallax lightfield rendering capability, which is anticipated to overcome the persisting accommodation-convergence discrepancy problem and to substantially reduce visual discomfort and fatigue experiences of users.

[0030] Full-parallax lightfield creation method. An important step to address the accommodation-convergence discrepancy problem is to provide the capability of correctly

rendering the focus cues of digital information regardless of its distance to the viewer, rather than rendering digital information on a fixed-distance 2D surface. Among the different non-stereoscopic display methods, we chose to use an InI method that allows the reconstruction of the full-parallax lightfields of a 3D scene appearing to be emitted by a 3D scene seen from constrained or unconstrained viewing zones. Compared with all other techniques, an InI technique requires a minimal amount of hardware complexity, which makes it possible to integrate it with an OST-HMD optical system and create a wearable true 3D AR display.

[0031] Figure 3 schematically illustrates an exemplary micro-InI unit 300. A set of 2D elemental images 301, each representing a different perspective of a 3D scene, are displayed on a high-resolution microdisplay 310. Through a microlens array (MLA) 320, each elemental image 301 works as a spatially-incoherent object and the conical ray bundles emitted by the pixels in the elemental images 301 intersect and integrally create the perception of a 3D scene, in which objects appear to be located along the surface AOB having a depth range Z_0 at a reference plane, for example, to provide the appearance to emit light and occupy the 3D space. The microlens array may be placed a distance "g" from the microdisplay 310 to create either a virtual or a real 3D scene. The micro-InI unit 300 allows the optical reconstruction of a 3D surface shape with full parallax information. It should be noted that an InI-based 3D display operates fundamentally differently from multi-view stereoscopic systems where a lenticular sheet functions as a spatial de-multiplexer to select appropriate discrete left-eye and right-eye planar views of a scene dependent on viewer positions. Such multi-view systems produce a defined number of binocular views typically with horizontal parallax only and may continue to suffer from convergence accommodation conflict.

[0032] Figure 4 schematically illustrates an alternative configuration of a micro-InI unit 400 in accordance with the present invention that creates a telecentric 3D lightfield of a 3D scene at surface AOB. A primary difference from the configuration of Figure 3 lies in the use of additional lenses (lens 430 and/or lens 440) which help to relay the apertures of a microlens array (MLA) 420 and creates a telecentric 3D lightfield. (R. Martínez-Cuenca, H. Navarro, G. Saavedra, B. Javidi, and M. Martínez-Corral, "Enhanced viewing-angle integral imaging by multiple-axis telecentric relay system," Optics Express, Vol. 15, Issue 24, pp. 16255-16260, 21 November 2007.) Lens 430 and lens 440 have the same focal distance, $f_1=f_2$, with lens 430 directly attached to the MLA 420 and lens 440 placed at a focal distance, f_1, away. The gap between the microdisplay 410 and the MLA 420 is the same as the focal distance, f_0,

of the MLA 420. The main advantages of this alternative design are the potential increase of viewing angle for the reconstructed 3D scene, compactness, ease of integration with the HMD viewing optics, and blocking of the flipped images created by rays refracted by microlenses 421 of the MLA 420 other than the correctly paired elemental image 401 and microlens 421.

[0033] Although the InI method is promising, improvements are still desirable due to three major limitations: (1) low lateral and longitudinal resolutions; (2) narrow depth of field (DOF); and (3) limited field of view angle. These limitations are subject to the limited imaging capability and finite aperture of microlenses, poor spatial resolution of large-size displays, and the trade-off relationship between wide view angle and high spatial resolution. Conventional InI systems typically yield low lateral and depth resolutions and narrow DOF. These limitations, however, can be alleviated in a wearable InI-HMD system of the present invention. First, microdisplays with large pixel counts and very fine pixels (e.g. ~5μm pixel size) may be used in the present invention to replace large-pixel display devices (~200-500μm pixel size) used in conventional InI displays, offering at least 50x gain in spatial resolution, Fig. 7. Secondly, due to the nature of HMD systems, the viewing zone is well confined and therefore a much smaller number of elemental images would be adequate to generate the full-parallax lightfields for the confined viewing zone than large-size auto-stereoscopic displays. Thirdly, to produce a perceived 3D volume spanning from 40cm to 5m depth range in an InI-HMD system, a very narrow depth range (e.g. Z_0 ~3.5mm) is adequate for the intermediate 3D scene reconstructed by the micro-InI unit, which is much more affordable than in a conventional stand-alone InI display system requiring at least 50cm depth range to be usable, Fig. 7. Finally, by optimizing the microlenses and the HMD viewing optics together, the depth resolution of the overall InI-HMD system can be substantially improved, overcoming the imaging limit of a stand-alone InI system.

[0034] The lightfields of the miniature 3D scene reconstructed by a micro-InI unit may be relayed by eyepiece optics into the eye for viewing. The eyepiece optics not only effectively couples the 3D lightfields into the eye (exit) pupil but may also magnify the 3D scene to create a virtual 3D display appearing to be at a finite distance from the viewer.

[0035] As an example, Figure 5 schematically illustrates the integration of a micro-InI unit 530 with conventional eyepiece optics 540. The micro-InI unit 530 may include a microdisplay 510 and microlens array 520 that may be configured in a similar manner to that illustrated in Fig. 3. The micro-InI unit 530 reconstructs a miniature 3D scene (located at

AOB in Fig. 5) which is located near the back focal point of the eyepiece optics 540. Through the eyepiece optics 540 the miniature scene may be magnified into an extended 3D display at A'O'B' which can then be viewed from a small zone constrained by the exit pupil of the eyepiece optics 540. Due to the 3D nature of the reconstructed scene, a different viewing perspective is seen at different locations within the exit pupil.

[0036] Among the different methods for HMD designs, freeform optical technology demonstrates great promise in designing compact HMD systems. Figure 6A illustrates the schematics of an exemplary configuration of a wearable 3D augmented reality display 600 in accordance with the present invention. The wearable 3D augmented reality display 600 includes a 3D InI unit 630 and a freeform eyepiece 640. The micro-InI unit 630 may include a microdisplay 610 and microlens array 620 that may be configured in a similar manner to that illustrated in Fig. 3. This configuration 600 adopts a wedge-shaped freeform prism as the eyepiece 640, through which the 3D scene reconstructed by the micro-InI unit 630 is magnified and viewed. Such eyepiece 640 is formed by three freeform optical surfaces which are labeled as 1, 2, and 3, respectively, which may be rotationally asymmetric surfaces. The exit pupil is where the eye is placed to view the magnified 3D scene, which is located of the virtual reference plane conjugate to the reference plane of the 3D InI unit 630. A light ray emitted from a 3D point (e.g. A) located at the intermediate scene is first refracted by the surface 3 of the freeform eyepiece 640 located closest to the reference plane. Subsequently, the light ray experiences two consecutive reflections by the surfaces 1' and 2, and finally is transmitted through the surface 1 and reaches the exit pupil of the system. Multiple ray directions from the same object point (e.g. each of the 3 rays from point A), each of which represents a different view of the object, impinge on different locations of the exit pupil and reconstruct a virtual 3D point (e.g. A') in front of the eye.

[0037] Rather than requiring multiple elements, the optical path is naturally folded within a three-surface prism structure of the eyepiece 640, which helps reduce the overall volume and weight of the optics substantially when compared with designs using rotationally symmetric elements.

[0038] To enable see-through capability for AR systems, surface 2 of the eyepiece 640 may be coated as a beam splitting mirror. A freeform corrector lens 650 may be added to provide a wearable 3D augmented reality display 690 having improved see-through capability. The corrector lens 650 may include two freeform surfaces which may be attached to the surface 2 of the eyepiece 640 to correct the viewing axis deviation and undesirable aberrations

introduced by the freeform prism eyepiece 640 to the real world scene. The rays from the virtual lightfield generated by the 3D InI unit 630 are reflected by surface 2 of the prism eyepiece 640, while the rays from a real-world scene are transmitted through the freeform eyepiece 640 and corrector lens 650, Fig. 6C. Figure 6C schematically illustrates the integration and raytracing of the overall wearable 3D augmented reality display 690. The front surface of the freeform corrector lens 650 matches the shape of surface 2 of the prism eyepiece 640. The back surface 4 of the corrector lens 650 may be optimized to minimize the shift and distortion introduced to the rays from a real-world scene when the corrector lens 650 is combined with the prism eyepiece 640. The additional corrector lens 650 is not expected to noticeably increase the footprint and weight of the overall system 690.

[0039] Thus, in devices of the present invention, the freeform eyepiece 640 may image the lightfield of a 3D surface AOB, rather than a 2D image surface. In such an InI-HMD system 600, 690, the freeform eyepiece 640 can reconstruct the lightfield of a virtual 3D object A'O'B' at a location optically conjugate to the lightfield of a real object, while in a conventional HMD system the eyepiece creates a magnified 2D virtual display which is optically conjugate to the 2D microdisplay surface.

[0040] In another of its aspects, the present invention may provide a 3D augmented reality optical see-through HMD 700 in which the location of the virtual reference plane may be adjusted, Fig. 6D. The ability to adjust the location of the virtual reference plane may be particularly useful in addressing the accommodation-convergence discrepancy by selecting the location of the virtual reference plane containing the augmented reality information relative to the location of objects in the real world scene being observed by the viewer. In this regard, Figure 6D schematically illustrates an alternative configuration of a 3D augmented reality optical see-through HMD 700 in accordance with the present invention which integrates a vari-focal element 728 in the optical path of a micro-InI module 730. As with the design of Fig. 6C, the HMD 700 may include an eyepiece 640, corrector lens 650, and a micro-InI unit 730 with a microdisplay 710 and microlens array 720, which may be identical to those used in Fig. 6C.

[0041] The optical power of the vari-focal element 728 (VFE) may be varied by applying an electrical voltage to the element. Examples of vari-focal elements 728 that may be used include liquid crystal lenses, liquid lenses, membrane mirrors, or birefringent lenses. Having the ability to dynamically change the optical power of the micro-InI unit 730 not only allows dynamic control of the axial position of the reference plane of the 3D reconstructed scene, but

also enables dynamic adjustment of the view angle of the reconstructed scene. For instance, varying the voltage on the VFE 728 allows one to place the virtual reference plane at a distance as close as 25cm (e.g. at O') or as far as optical infinity (e.g. at O'') or vice versa without having to make mechanical changes. Varying the optical power of the VFE 728 also enables dynamic control on the ray angles of the light reconstructing the 3D scene and thus controls the viewing angle. This capability enabled through the VFE 728 allows one to improve the longitudinal resolution, extend the depth of field, and increase viewing angles. The change of optical power on the VFE 728 may be controlled by the knowledge of the 3D scene depth to be rendered, or the knowledge of the user's region of interest. For instance, knowing the absolute depth of the reconstructed virtual scene (e.g. A'O'B') with respect to the viewer and the depth range of the scene allows the system to properly position the virtual reference plane with optimal longitudinal resolution and viewing angle. Alternatively, the region of interest of the viewer, which may be detected through an eye movement tracking device, may be dynamically acquired and utilized to position the virtual reference plane accordingly. When both the VFE 728 and the microdisplay 710 operate at high speed (e.g., at least twice the critical flickering frequency of the human visual system), 3D scenes of different depths can be rendered time sequentially with the reference plane placed over these depths to cover an extended depth volume. The time-sequentially rendered scenes may then be viewed as a continuous 3D volume due to the advantage of the speed. A liquid crystal lens 728 may be used for varying the depth of field of the integral imaging display. Other types of spatial light modulators may be used as well such as deformable mirror devices for high speed modulation.

[0042] In yet another of its aspects, the present invention may provide a 3D augmented reality optical see-through HMD 800 which integrates three-dimensional (3D) or 2D object recognition capability, Fig. 6E. For example, Figure 6E schematically illustrates an alternative configuration of a 3D augmented reality optical see-through HMD 800 in accordance with the present invention which integrates three-dimensional (3D) or 2D object recognition capability with augmented reality (AR). As with the design of Fig. 6C, the HMD 800 may include an eyepiece 640, corrector lens 650, and a micro-InI unit 830 with a microdisplay 810 and microlens array 820, which may be identical to those used in Fig. 6C. The HMD 800 may combine an integral imaging optical 3D display method and 2D/3D object recognition capability by attaching at least one camera 815 to the HMD 800, Fig. 6E. The current state of the art allows the availability of light weight mega pixel cameras as small

as one millimeter square. (Sony 960H Micro Pinhole Covert Camera #20-100.) The camera 815 may be a regular video camera, but more importantly it can be a 3D integral imaging image capture system where a micro lenslet array is utilized in the imaging optics to capture the 3D lightfield of the real-world scene 10. Using the images captured by such a camera 815, one can implement either 2D imaging or 3D integral imaging acquisition, numerical visualization, and 2D or 3D object recognition, segmentation, and localization of objects in the scene 10. While the real scene 10 is observed by the user directly through the free form optics 640, 650, object recognition capability enabled by the capture unit 850 can allow the intelligent extraction of information about the detected objects and scene, their description, their position, their range using (3D imaging properties of integral imaging), their relation with other objects in the scene, etc and such information can be presented to the viewer through augmenting of the reality. For example, if the viewer is looking for a particular object in a crowded scene, the recognition capability can detect this object and present it, including its location to the viewer using AR. A variety of architectures can be used for the 3D object visualization, which may be run on a general purpose computer to provide the capture unit 850. (S. Hong, J. Jang, and B. Javidi, "Three-dimensional volumetric object reconstruction using computational integral imaging," Journal of Optics Express, on-line Journal of the Optical Society of America, Vol. 12, No. 3, pp. 483-491, February 09, 2004. R. Schulein, M. DaneshPanah, and B. Javidi, "3D imaging with axially distributed sensing," Journal of Optics Letters, Vol. 34, Issue 13, pp. 2012-2014, 1 July 2009) or recognition. (S. Kishk and B. Javidi, "Improved Resolution 3D Object Sensing and Recognition using time multiplexed Computational Integral Imaging," Optics Express, on-line Journal of the Optical Society of America, vol. 11, no. 26, pp. 3528-3541, December 29, 2003. R. Schulein, C. Do, and B. Javidi, "Distortion-tolerant 3D recognition of underwater objects using neural networks," Journal of Optical Society of America A, vol. 27, no. 3, pp 461-468, March 2010. C. Manh Do, R. Martínez-Cuenca, and B. Javidi, "Three-dimensional object-distortion-tolerant recognition for integral imaging using independent component analysis," Journal of Optical Society of America A 26, issue 2, pp 245-251 (1 February 2009). S. Hong and B. Javidi, "Distortion-tolerant 3D recognition of occluded objects using computational integral imaging," Journal of Optics Express, Vol. 14, Issue 25, pp. 12085-12095, December 11, 2006.). A variety of algorithms can be used for 2D or 3D object recognition. (F. Sadjadi and B. Javidi, "Physics of Automatic Target Recognition," Springer-Verlag, New York, 2007. R. J. Schalkoff, Pattern Recognition: Statistical,

Structural and Neural Approaches (Wiley, 1991). Christopher M. Bishop, Neural Networks for Pattern Recognition, Oxford University Press, Inc. New York, NY 1995. A. K. Jain, Fundamentals of Digital Image Processing, Prentice Hall. M. Daneshpanah, B. Javidi, and E. Watson, "Three dimensional integral imaging with randomly distributed sensors," Journal of Optics Express, Vol. 16, Issue 9, pp. 6368-6377, April 21, 2008. R. Schulein, M. DaneshPanah, and B. Javidi, "3D imaging with axially distributed sensing," Journal of Optics Letters, Vol. 34, Issue 13, pp. 2012-2014, 1 July 2009). It is possible to have a 3D object recognition capability by using a single camera 815 when the viewer is moving. Or, it is possible to have a 3D object recognition capability by using a single camera 815 with zero parallax by using axially distributed sensing when the viewer is moving towards the object.

Examples

[0043] A proof-of-concept monocular prototype of an InI OST-HMD according to the configuration of Fig. 6C was implemented using off-the-shelf optical components, Fig. 8. A micro-lens array (MLA) of a 3.3mm focal length and 0.985mm pitch was utilized. (These types of microlenses can be purchased from Digital Optics Corp, SUSS Microoptics, etc.) The microdisplay was a 0.8" organic light emitting display (OLED), which offered 1920x1200 color pixels with a pixel size of 9.6μm. (EMA-100820, by eMagin Corp, Bellevue, WA.) A freeform eyepiece along with a see-through corrector were used of the type disclosed in International Patent Application No. PCT/US2013/065422, the entire contents of which are incorporated herein by reference. The specifications of the eyepiece 640 and corrector 650 are provided in the tables below. The eyepiece offered a field of view of 40 degrees and approximately a 6.5mm eyebox. Due to the strict telecentricity of the eyepiece design, it was adapted to the InI setup with reasonably low crosstalk but with a narrow viewing zone. It is worth noting that adapting this particular freeform eyepiece design is not required for implementing the optical method described in this invention. Alternative eyepieces may be designed and optimized for this purpose.

System prescription for display path

[0044] In **Error! Reference source not found.**1, surfaces #2 – #4 specify the free-form eyepiece 640. Table 1 surfaces #2 and #4 represent the same physical surface and corresponds to eyepiece surface 1, in Figs. 6A–6C. Table 1 surface #3 is corresponds eyepiece surface 2, and Table 1 surface #5 corresponds to eyepiece surface 3, in Figs. 6A–6C.

Surface No.	Surface Type	Y Radius	Thickness	Material	Refract Mode
1 (Stop)	Sphere	Infinity	0.000		Refract
2	XY Poly	-185.496	0.000	PMMA	Refract
3	XY Poly	-67.446	0.000	PMMA	Reflect
4	XY Poly	-185.496	0.000	PMMA	Reflect
5	XY Poly	-830.046	0.000		Refract
6	Sphere	Infinity	0.000		Refract

Table 1. Surface prescription of eyepiece – AR display path.

Surface No.	Surface Type	Y Radius	X Radius	Thick -ness	Material	Refract Mode
1 (Stop)	Sphere	Infinity	Infinity	0.000		Refract
2	XY Poly	-185.496	-185.496	0.000	PMMA	Refract
3	XY Poly	-67.446	-67.446	0.000	PMMA	Refract
4	XY Poly	-67.446	-67.446	0.000	PMMA	Refract
5	XY Poly	-87.790	-87.790	10.00		Refract
6	Cylindrical	Infinity	-103.400	6.5	NBK7	Refract
7	Sphere	Infinity	Infinity	0.000		Refract

Table 2. System prescription for see-through path.

System prescription for optical see-through path

[0045] In Table 2 surfaces #2 and #3 are eyepiece surfaces 1 and 3, modeled the same as in the display path. Surfaces #4, #5 specify the freeform corrector lens 650. Surface #4 is an exact replica of Surface #3 (eyepiece surface 2).

Y Radius	-1.854965E+02	**X**2 * Y**5**	-1.505674E-10
Conic Constant	-2.497467E+01	**X * Y**6**	0.000000E+00
X	0.000000E+00	**Y**7**	-4.419392E-11
Y	0.000000E+00	**X**8**	4.236650E-10
X2**	-2.331157E-03	**X**7 * Y**	0.000000E+00
X * Y	0.000000E+00	**X**6 * Y**2**	-1.079269E-10
Y2**	6.691726E-04	**X**5 * Y**3**	0.000000E+00
X3**	0.000000E+00	**X**4 * Y**4**	-1.678245E-10
X2 * Y**	-1.066279E-04	**X**3 * Y**5**	0.000000E+00
X Y2**	0.000000E+00	**X**2 * Y**6**	2.198604E-12
Y3**	-2.956368E-05	**X * Y**7**	0.000000E+00
X4**	-1.554280E-06	**Y**8**	-2.415118E-12
X3 * Y**	0.000000E+00	**X**9**	0.000000E+00
X2 * Y**2**	1.107189E-06	**X**8 * Y**	4.113054E-12
X * Y3**	0.000000E+00	**X**7 * Y**2**	0.000000E+00
Y4**	1.579876E-07	**X**6 * Y**3**	-1.805964E-12
X5**	0.000000E+00	**X**5 * Y**4**	0.000000E+00
X4 * Y**	1.789364E-07	**X**4 * Y**5**	9.480632E-13
X3 * Y**2**	0.000000E+00	**X**3 * Y**6**	0.000000E+00
X2 * Y**3**	-2.609879E-07	**X**2 * Y**7**	2.891726E-13
X * Y4**	0.000000E+00	**X * Y**8**	0.000000E+00
Y5**	-6.129549E-10	**Y**9**	-2.962804E-14
X6**	-3.316779E-08	**X**10**	-6.030361E-13
X5 * Y**	0.000000E+00	**X**9 * Y**	0.000000E+00
X4 * Y**2**	9.498635E-09	**X**8 * Y**2**	-7.368710E-13
X3 * Y**3**	0.000000E+00	**X**7 * Y**3**	0.000000E+00
X2 * Y**4**	9.042084E-09	**X**6 * Y**4**	9.567750E-13
X * Y5**	0.000000E+00	**X**5 * Y**5**	0.000000E+00
Y6**	-4.013470E-10	**X**4 * Y**6**	4.280494E-14
X7**	0.000000E+00	**X**3 * Y**7**	0.000000E+00
X6 * Y**	-8.112755E-10	**X**2 * Y**8**	-7.143578E-15
X5 * Y**2**	0.000000E+00	**X * Y**9**	0.000000E+00
X4 * Y**3**	1.251040E-09	**Y**10**	3.858414E-15
X3 * Y**4**	0.000000E+00	**N-Radius**	1.000000E+00

Table 3. Optical surface prescription of Surface #2 and #4 of Table 1.

Y DECENTER	Z DECENTER	ALPHA TILT
6.775E+00	2.773E+01	7.711E+00

Table 4. Decenter of Surface #2 and #4 of Table 1, relative to Surface #1 of Table 1.

Y Radius	-6.744597E+01	**X**2 * Y**5**	-3.464751E-11
Conic Constant	-1.258507E+00	**X * Y**6**	0.000000E+00
X	0.000000E+00	**Y**7**	-8.246179E-12
Y	0.000000E+00	**X**8**	-2.087865E-11
X2**	-1.300207E-03	**X**7 * Y**	0.000000E+00
X * Y	0.000000E+00	**X**6 * Y**2**	2.845323E-11
Y2**	4.658585E-04	**X**5 * Y**3**	0.000000E+00
X3**	0.000000E+00	**X**4 * Y**4**	-5.043398E-12
X2 * Y**	-1.758475E-05	**X**3 * Y**5**	0.000000E+00
X Y2**	0.000000E+00	**X**2 * Y**6**	2.142939E-14
Y3**	-1.684923E-06	**X * Y**7**	0.000000E+00
X4**	-1.463720E-06	**Y**8**	1.607499E-12
X3 * Y**	0.000000E+00	**X**9**	0.000000E+00
X2 * Y**2**	-1.108359E-06	**X**8 * Y**	-1.922597E-12
X * Y3**	0.000000E+00	**X**7 * Y**2**	0.000000E+00
Y4**	-1.098749E-07	**X**6 * Y**3**	1.100072E-13
X5**	0.000000E+00	**X**5 * Y**4**	0.000000E+00
X4 * Y**	-7.146353E-08	**X**4 * Y**5**	-4.806130E-14
X3 * Y**2**	0.000000E+00	**X**3 * Y**6**	0.000000E+00
X2 * Y**3**	-1.150619E-08	**X**2 * Y**7**	-2.913177E-14
X * Y4**	0.000000E+00	**X * Y**8**	0.000000E+00
Y5**	5.911371E-09	**Y**9**	9.703717E-14
X6**	-5.406591E-10	**X**10**	2.032150E-13
X5 * Y**	0.000000E+00	**X**9 * Y**	0.000000E+00
X4 * Y**2**	-1.767107E-09	**X**8 * Y**2**	-1.037107E-13
X3 * Y**3**	0.000000E+00	**X**7 * Y**3**	0.000000E+00
X2 * Y**4**	-7.415334E-10	**X**6 * Y**4**	3.602862E-14
X * Y5**	0.000000E+00	**X**5 * Y**5**	0.000000E+00
Y6**	-5.442400E-10	**X**4 * Y**6**	-8.831469E-15
X7**	0.000000E+00	**X**3 * Y**7**	0.000000E+00
X6 * Y**	6.463414E-10	**X**2 * Y**8**	2.178095E-15
X5 * Y**2**	0.000000E+00	**X * Y**9**	0.000000E+00
X4 * Y**3**	1.421597E-10	**Y**10**	1.784074E-15
X3 * Y**4**	0.000000E+00	**N-Radius**	1.000000E+00

Table 5. Optical surface prescription of Surface #3 of Table 1.

Y DECENTER	Z DECENTER	ALPHA TILT
1.329E+01	4.321E+01	-8.856E+00

Table 6. Decenter of Surface #3 of Table 5 relative to Surface #1 of Table 1.

Y Radius	-8.300457E+02	**X**2 * Y**5**	4.051880E-08
Conic Constant	-9.675799E+00	**X * Y**6**	0.000000E+00
X	0.000000E+00	**Y**7**	-3.973293E-09
Y	0.000000E+00	**X**8**	-1.881791E-10
X2**	-1.798206E-04	**X**7 * Y**	0.000000E+00
X * Y	0.000000E+00	**X**6 * Y**2**	5.519986E-09
Y2**	-2.606383E-03	**X**5 * Y**3**	0.000000E+00
X3**	0.000000E+00	**X**4 * Y**4**	3.822268E-09
X2 * Y**	-7.767146E-05	**X**3 * Y**5**	0.000000E+00
X Y2**	0.000000E+00	**X**2 * Y**6**	-3.024448E-09
Y3**	-8.958581E-05	**X * Y**7**	0.000000E+00
X4**	1.978414E-05	**Y**8**	2.673713E-11
X3 * Y**	0.000000E+00	**X**9**	0.000000E+00
X2 * Y**2**	2.081156E-05	**X**8 * Y**	1.006915E-10
X * Y3**	0.000000E+00	**X**7 * Y**2**	0.000000E+00
Y4**	-1.073001E-06	**X**6 * Y**3**	-2.945084E-10
X5**	0.000000E+00	**X**5 * Y**4**	0.000000E+00
X4 * Y**	2.585164E-07	**X**4 * Y**5**	5.958040E-10
X3 * Y**2**	0.000000E+00	**X**3 * Y**6**	0.000000E+00
X2 * Y**3**	-2.752516E-06	**X**2 * Y**7**	-3.211903E-10
X * Y4**	0.000000E+00	**X * Y**8**	0.000000E+00
Y5**	-1.470053E-06	**Y**9**	2.296303E-11
X6**	-1.116386E-07	**X**10**	5.221834E-12
X5 * Y**	0.000000E+00	**X**9 * Y**	0.000000E+00
X4 * Y**2**	-3.501439E-07	**X**8 * Y**2**	1.135044E-11
X3 * Y**3**	0.000000E+00	**X**7 * Y**3**	0.000000E+00
X2 * Y**4**	1.324057E-07	**X**6 * Y**4**	-1.050621E-10
X * Y5**	0.000000E+00	**X**5 * Y**5**	0.000000E+00
Y6**	-9.038017E-08	**X**4 * Y**6**	5.624902E-11
X7**	0.000000E+00	**X**3 * Y**7**	0.000000E+00
X6 * Y**	3.397174E-10	**X**2 * Y**8**	5.369592E-12
X5 * Y**2**	0.000000E+00	**X * Y**9**	0.000000E+00
X4 * Y**3**	-1.873966E-08	**Y**10**	2.497657E-12
X3 * Y**4**	0.000000E+00	**N-Radius**	1.000000E+00

Table 7. Optical surface prescription of Surface #5 of Table 1.

Y DECENTER	Z DECENTER	ALPHA TILT
.427E+01	3.347E+01	7.230E+01

Table 8. Decenter of Surface #5 relative to Surface #1 of Table 1.

Y Radius	-8.779024E+01	**X**2 * Y**5**	-8.011955E-11
Conic Constant	-7.055198E+00	**X * Y**6**	0.000000E+00
X	0.000000E+00	**Y**7**	3.606142E-11
Y	0.000000E+00	**X**8**	3.208020E-11
X2**	-3.191225E-03	**X**7 * Y**	0.000000E+00
X * Y	0.000000E+00	**X**6 * Y**2**	-2.180416E-11
Y2**	4.331992E-03	**X**5 * Y**3**	0.000000E+00
X3**	0.000000E+00	**X**4 * Y**4**	-3.616135E-11
X2 * Y**	-9.609025E-05	**X**3 * Y**5**	0.000000E+00
X Y2**	0.000000E+00	**X**2 * Y**6**	-5.893434E-12
Y3**	-2.432809E-05	**X * Y**7**	0.000000E+00
X4**	-2.955089E-06	**Y**8**	3.081069E-12
X3 * Y**	0.000000E+00	**X**9**	0.000000E+00
X2 * Y**2**	2.096887E-07	**X**8 * Y**	1.267096E-12
X * Y3**	0.000000E+00	**X**7 * Y**2**	0.000000E+00
Y4**	-9.184356E-07	**X**6 * Y**3**	-1.848104E-12
X5**	0.000000E+00	**X**5 * Y**4**	0.000000E+00
X4 * Y**	3.707556E-08	**X**4 * Y**5**	5.208420E-14
X3 * Y**2**	0.000000E+00	**X**3 * Y**6**	0.000000E+00
X2 * Y**3**	-1.535357E-07	**X**2 * Y**7**	1.198597E-13
X * Y4**	0.000000E+00	**X * Y**8**	0.000000E+00
Y5**	-1.445904E-08	**Y**9**	-6.834914E-14
X6**	-4.440851E-09	**X**10**	-1.706677E-14
X5 * Y**	0.000000E+00	**X**9 * Y**	0.000000E+00
X4 * Y**2**	1.686424E-09	**X**8 * Y**2**	-1.614840E-14
X3 * Y**3**	0.000000E+00	**X**7 * Y**3**	0.000000E+00
X2 * Y**4**	6.770909E-09	**X**6 * Y**4**	8.739087E-14
X * Y5**	0.000000E+00	**X**5 * Y**5**	0.000000E+00
Y6**	-3.713094E-10	**X**4 * Y**6**	3.940903E-15
X7**	0.000000E+00	**X**3 * Y**7**	0.000000E+00
X6 * Y**	-1.316067E-10	**X**2 * Y**8**	5.435162E-15
X5 * Y**2**	0.000000E+00	**X * Y**9**	0.000000E+00
X4 * Y**3**	7.924387E-10	**Y**10**	-2.259169E-15
X3 * Y**4**	0.000000E+00	**N-Radius**	1.000000E+00

Table 9. Optical surface prescription of Surface #5 of Table 2.

Y DECENTER	Z DECENTER	ALPHA TILT
3.358E+00	4.900E+01	6.765E+00

Table 10. Decenter of Surface #5 relative to Surface #1 of Table 2.

[0046] As used in the system prescription Tables, *e.g.*, Table 1 or **Error! Reference source not found.**2, the term "XY Poly" refers to a surface which may be respresented by the equation

$$z = \frac{cr^2}{1+\sqrt{1-(1+k)c^2r^2}} + \sum_{j=2}^{66} C_j x^m y^n \qquad j = \frac{(m+n)^2 + m + 3n}{2} + 1,$$

where z is the sag of the free-form surface measured along the z-axis of a local x, y, z coordinate system, c is the vertex curvature (CUY), r is the radial distance, k is the conic constant, and C_j is the coefficient for $x^m y^n$.

[0047] For demonstration purposes, a 3D scene including a number "3" and a letter "D" was simulated. In the visual space, the objects "3" and "D" were located ~4 meters and 30cms away from the eye position, respectively. To clearly demonstrate the effects of focusing, these character objects, instead of using plain solid colors, were rendered with black line textures. An array of 18x11 elemental images of the 3D scene were simulated (Fig. 9), each of which consisted of 102 by 102 color pixels. The 3D scene reconstructed by the micro-InI unit was approximately 10mm away from the MLA and the separation of the two reconstructed targets was approximately 3.5 mm in depth in the intermediate reconstruction space.

[0048] Figures 10A through 10D shows a set of images captured with a digital camera placed at the eye position. To demonstrate the effects of focus and see-through view, in the real-world view, a Snellen letter chart and a printed black-white grating target were placed ~4 meters and 30 cm away from the viewer, respectively, which corresponded to the locations of the objects "3" and "D", respectively.

[0049] Figures 10A and 10B demonstrate the effects of focusing the camera on the Snellen chart and grating target, respectively. The object "3" appeared to be in sharp focus when the camera was focused on the far Snellen chart while the object "D" was in focus when the camera was focused on the near grating target. Figures 10C and 10D demonstrate the effects of shifting the camera position from the left to the right sides of the eyebox while the camera focus was set on the near grating target. As expected, slight perspective change was observed between these two views. Although artifacts admittedly are visible and further development is needed, the results clearly demonstrated that the proposed method for AR display can produce correct focus cues and true 3D viewing in a large depth range.

[0050] The invention described and claimed herein is not to be limited in scope by the specific embodiments herein disclosed, since these embodiments are intended as illustrations of several aspects of the invention. Any equivalent embodiments are intended to be within the scope of this invention. Indeed, various modifications of the invention in addition to those shown and described herein will become apparent to those skilled in the art from the foregoing description. Such modifications are also intended to fall within the scope of the appended claims.

[0051] A number of patent and non-patent publications are cited in the specification, the entire disclosure of each of these publications is incorporated by reference herein.

References

[1] Yano, S., Emoto, M., Mitsuhashi, T., and Thwaites, H., "A study of visual fatigue and visual comfort for 3D HDTV/HDTV images," Displays, 23(4), pp. 191-201, 2002.

[2] S.J. Watt, K. Akeley, M.O. Ernst, and M.S. Banks, "Focus Cues Affect Perceived Depth," J. Vision, 5(10), 834-862, (2005).

[3] D.M. Hoffman, A.R. Girshick, K. Akeley, and M.S. Banks, "Vergence-Accommodation Conflicts Hinder Visual Performance and Cause Visual Fatigue," J. Vision, 8(3), 1-30, (2008).

[4] G. Lippmann, "Epreuves reversibles donnant la sensation du relief," Journal of Physics (Paris) 7, 821–825 (1908).

[5] C. B. Burckhardt, "Optimum parameters and resolution limitation of integral photography," J. Opt. Soc. Am. 58, 71–76 (1968).

[6] T. Okoshi, "Optimum design and depth resolution of lens-sheet and projection-type three-dimensional displays," Appl. Opt. 10, 2284–2291 (1971).

[7] F. Okano, H. Hoshino, J. Arai y I. Yuyama, "Real-time pickup method for a three-dimensional image based on integral photography," Appl. Opt. 36, 1598–1603 (1997).

[8] J. Aran, "Depth-control method for integral imaging," Optics Letters, 33(3): 279-282, 2008.

[9] H. Hua, "Sunglass-like displays become a reality with freeform optical technology," SPIE Newsroom, 2012.

[10] H. Hua and C. Gao, A compact, eye-tracked optical see-through head-mounted display, Proc. SPIE 8288, p. 82881F, 2012.

[11] H. Hua, X. Hu, and C. Gao, "A high-resolution optical see-through head-mounted display with eyetracking capability," Optics Express, November 2013.

[12] D. Cheng, Y.Wang, H. Hua, and M. M. Talha, Design of an optical see-through headmounted display with a low f-number and large field of view using a free-form prism, App. Opt. 48 (14), pp. 2655–2668, 2009.

[13] D. Cheng, Y.Wang, H. Hua, and J. Sasian, Design of a wide-angle, lightweight headmounted display using free-form optics tiling, Opt. Lett. 36 (11), pp. 2098–2100, 2011.

[14] A. Okuyama and S. Yamazaki, Optical system and image observing apparatus and image pickup apparatus using it, US Patent 5,706,136, 1998.

[15] S. Yamazaki, K. Inoguchi, Y. Saito, H. Morishima, and N. Taniguchi, Thin widefield-of-view HMD with free-form-surface prism and applications, Proc. SPIE 3639,p. 453, 1999.

[16] A. Jones, I. McDowall, Yamada H., M. Bolas, P. Debevec, Rendering for an Interactive 360º Light Field Display ACM Transactions on Graphics (TOG) –Proceedings of ACM SIGGRAPH 2007, 26(3), 2007.

[17] Tibor Balogh, "The HoloVizio System," Proceedings of SPIE, VOl 6055, 2006.

[18] Y. Takaki, Y. Urano, S. Kashiwada, H. Ando, and K. Nakamura, "Super multi-view winshield display for long-distance image information presentation," Opt. Express, 19, 704-16, 2011.

[19] Blundell, B. G., and Schwarz, A. J., "The classification of volumetric display systems: characteristics and predictability of the image space," IEEE Transaction on Visualization and Computer Graphics, 8(1), pp. 66-75, 2002.

[20] P.A. Blanche, et al, "Holographic three-dimensional telepresence using large-area photorefractive polymer", Nature, 468, 80-83, Nov. 2010.

[21] Rolland, J. P., Kureger, M., and Goon, A., "Multifocal planes head-mounted displays," Applied Optics, 39(19), pp. 3209-14, 2000.

[22] Akeley, K., Watt, S., Girshick, A., and Banks, M., "A stereo display prototype with multiple focal distances," Proc. of SIGGRAPH, pp. 804-813, 2004.

[23] Schowengerdt, B. T., and Seibel, E. J., "True 3-D scanned voxel displays using single or multiple light sources," Journal of SID, 14(2), pp. 135-143, 2006.

[24] S. Liu, H. Hua, D. Cheng, "A Novel Prototype for an Optical See-Through Head-Mounted Display with Addressable Focus Cues," IEEE Transactions on Visualization and Computer Graphics, 16(3), 381-393, (2010).

[25] S. Liu and H. Hua, "A systematic method for designing depth-fused multi-focal plane three-dimensional displays," Opt. Express, 18, 11562-11573, (2010)

[26] X. Hu and H. Hua, "Design and assessment of a depth-fused multi-focal-plane display prototype," Journal of Display Technology, December 2013.

[27] Suyama, S., Ohtsuka, S., Takada, H., Uehira, K., and Sakai, S., "Apparent 3D image perceived from luminance-modulated two 2D images displayed at different depths," Vision Research, 44: 785-793, 2004.

[28] J. Hong, S. Min, and B. Lee, "Integral floating display systems for augmented reality," Applixed Optics, 51(18):4201-9, 2012.

[29] A. Malmone, and H. Fuchs, "Computational augmented reality eyeglasses," Proc. of ISMAR 2012.

[30] Rolland, J. P., and Hua, H., "Head-mounted display systems," in Encyclopedia of Optical Engineering (Editors: R. Barry Johnson and Ronald G. Driggers), New York, NY: Marcel Dekker, pp. 1-13, 2005.

[31] H. Mukawa, K. Akutsu, I. Matsumura, S. Nakano, T. Yoshida, M. Kuwahara, and K. Aiki, A full-color eyewear display using planar waveguides with reflection volume holograms, J. Soc. Inf. Display 19 (3), pp. 185–193, 2009.

[32] http://www.lumus-optical.com/

[33] http://www.innovega-inc.com

[34] http://www.epson.com/cgi-bin/Store/jsp/Moverio/Home.do

[35] http://www.google.com/glass/start/

[36] M. Martínez-Corral, H. Navarro, R. Martínez-Cuenca, G. Saavedra, and B. Javidi, "Full parallax 3-D TV with programmable display parameters," Opt. Phot. News 22, 50-50 (2011).

[37] J. S. Jang and B. Javidi, "Large depth-of-focus time-multiplexed three-dimensional integral imaging by use of lenslets with non-uniform focal lengths and aperture sizes," Opt. Lett. vol. 28, pp. 1924-1926 (2003).

[38] Chih-Wei Chen, Myungjin Cho, Yi-Pai Huang, and Bahram Javidi, "Improved viewing zones for projection type integral imaging 3D display using adaptive liquid crystal prism array," IEEE Journal of Display Technology, 2014.

[39] Xiao Xiao, Bahram Javidi, Manuel Martinez-Corral, and Adrian Stern , "Advances in Three-Dimensional Integral Imaging: Sensing, Display, and Applications," Applied Optics, 52(4):. 546–560,2013.

[40] J.S. Jang, F. Jin, and B. Javidi, "Three-dimensional integral imaging with large depth of focus by use of real and virtual image fields," Opt. Lett. 28:1421-23, 2003.

[41] S. Bagheri and B. Javidi, "Extension of Depth of Field Using Amplitude and Phase Modulation of the Pupil Function," Journal of Optics Letters, vol. 33, no. 7, pp. 757-759, 1 April 2008.

Claims

What is claimed is:

1. A 3D augmented reality display, comprising:
   a microdisplay for providing a virtual 3D image for display to a user;
   variable focus display optics configured to receive optical radiation from the microdisplay and configured to create a 3D lightfield from the received radiation at a location that may be varied by the variable focus optics; and
   an eyepiece in optical communication with the display optics configured to receive the 3D lightfield from the display optics and deliver the received radiation to an exit pupil of the augmented reality display.
2. The 3D augmented reality display of claim 1, wherein the variable focus display optics includes one or more of a liquid crystal lens, a liquid lens, a membrane mirror, or birefringent lens.
3. The 3D augmented reality display of any one of the preceding claims, comprising an imaging device configured to receive information from a scene.
4. A 3D augmented reality display, comprising:
   a microdisplay for providing a virtual 3D image for display to a user;
   display optics configured to receive optical radiation from the microdisplay and configured to create a 3D lightfield from the received radiation;
   an eyepiece in optical communication with the display optics configured to receive the 3D lightfield from the display optics and deliver the received radiation to an exit pupil of the augmented reality display; and
   an imaging device configured to receive information from a scene.
5. The 3D augmented reality display of anyone of claims 3–4, wherein the imaging device comprises a camera.
6. The 3D imaging augmented reality display of anyone of claims 3–5, wherein the imaging device comprises an integral imaging image capture system.
7. The 3D imaging augmented reality display of anyone of claims 3–6, wherein the imaging device comprises a 3D imaging capture system using axially distributed imaging.

8. The 3D augmented reality display of anyone of claims 3–7, wherein the imaging device includes an information capture unit for analyzing the information received by the imaging device to perform object recognition thereon.
9. The 3D augmented reality display of anyone of claims 3–8, wherein the imaging device is disposed in communication with the microdisplay to provide the analysis to the microdisplay.
10. The 3D imaging augmented reality display and object recognition of anyone of the preceding claims, wherein the image capture device includes a variable focal length optics to provide enhanced performance in terms of depth of field.
11. The 3D augmented reality display of any one of the preceding claims, wherein the display optics comprises integral imaging optics.
12. The 3D augmented reality display of any one of the preceding claims, wherein the eyepiece comprises a selected surface configured to receive the 3D lightfield from the display optics and reflect the received radiation to the exit pupil, the selected surface also configured to receive optical radiation from a source other than the microdisplay and to transmit the optical radiation to the exit pupil.
13. The 3D augmented reality display of any one of the preceding claims, wherein the eyepiece comprises a freeform prism shape.
14. The 3D augmented reality display of any one of the preceding claims, wherein the eyepiece comprises a first surface configured to receive and refract optical radiation from the display optics and comprises a second surface configured to receive the refracted optical radiation from the first surface, the second surface configured to reflect the optical radiation to a third surface of the eyepiece, the third surface configured to reflect the optical radiation reflected from the second surface to the exit pupil.
15. The 3D augmented reality display of claim 11, comprising a corrector lens disposed adjacent the second surface of the eyepiece.
16. The 3D augmented reality display of any one of the preceding claims, wherein one or more of the surfaces of the eyepiece comprise a rotationally asymmetric surface.

17. The 3D augmented reality display of any one of the preceding claims, wherein the eyepiece comprises a wedge shape.

18. The 3D augmented reality display of any one of the preceding claims, wherein the eyepiece comprises a surface respresented by the equation

$$z = \frac{cr^2}{1+\sqrt{1-(1+k)c^2r^2}} + \sum_{j=2}^{66} C_j x^m y^n \qquad j = \frac{(m+n)^2 + m + 3n}{2} + 1,$$

where z is the sag of the free-form surface measured along the z-axis of a local x, y, z coordinate system, c is the vertex curvature (CUY), r is the radial distance, k is the conic constant, and C_j is the coefficient for $x^m y^n$.

19. The 3D augmented reality display of any one of the preceding claims, wherein the display optics comprises one or more of a holographic display, multi-layer computational lightfield display, and a volumetric display.

20. The 3D imaging augmented reality display of any one of the preceding claims, wherein the 3D lightfield provides full parallax.

21. The 3D imaging augmented reality display of any one of the preceding claims, wherein the 3D lightfield provides partial parallax.

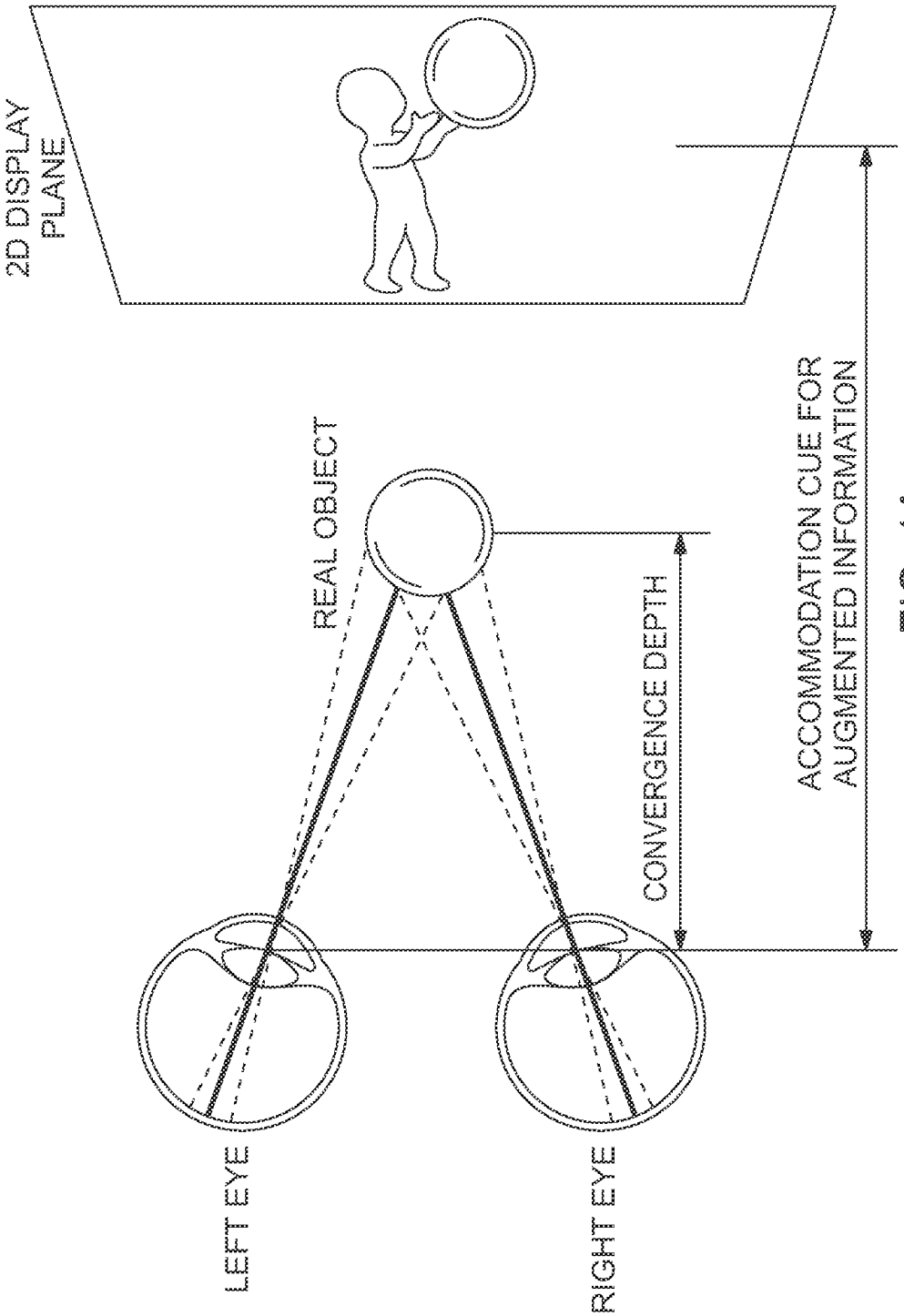
2D DISPLAY PLANE
REAL OBJECT
CONVERGENCE DEPTH
ACCOMMODATION CUE FOR AUGMENTED INFORMATION
LEFT EYE
RIGHT EYE

FIG. 1A

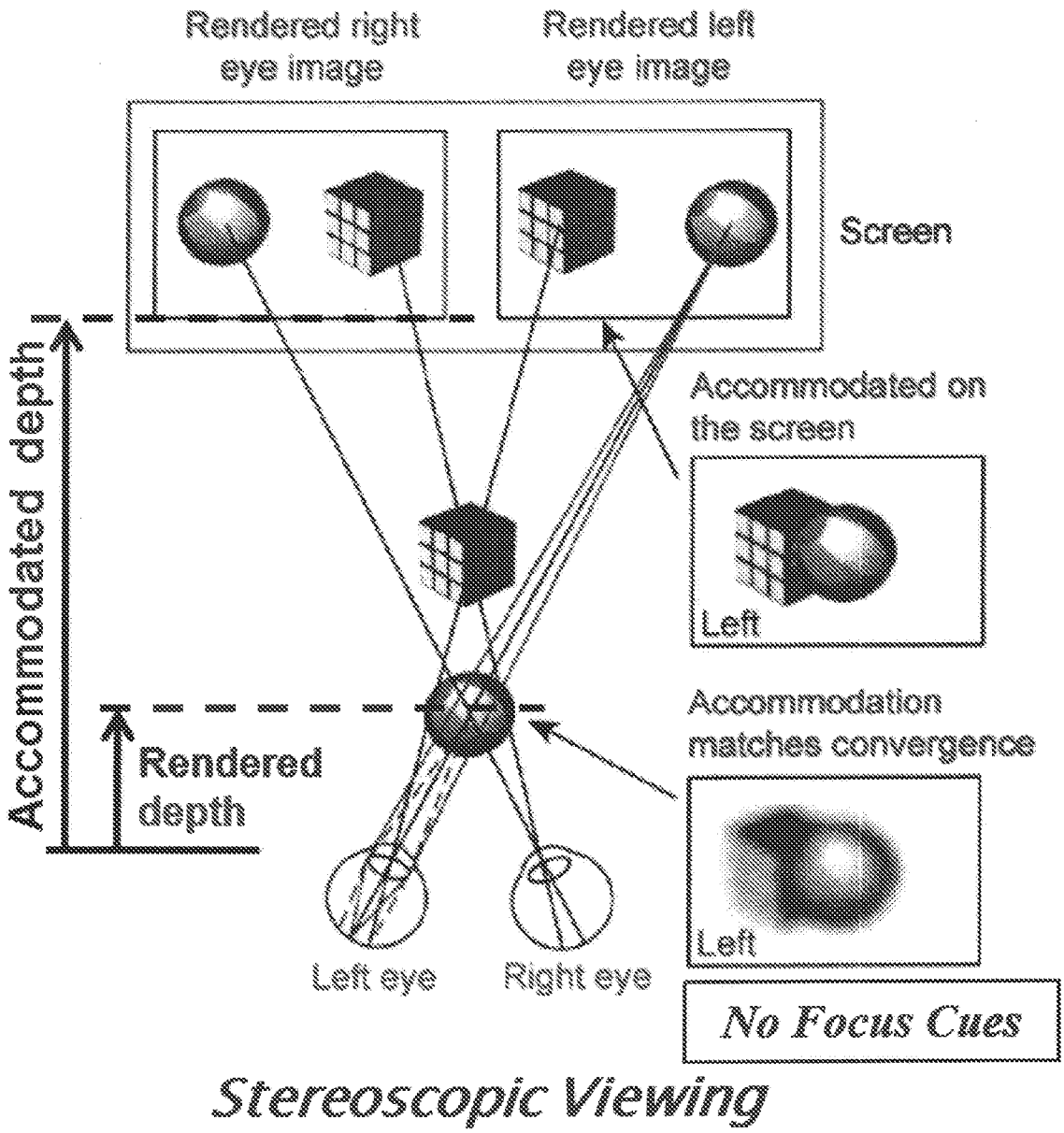
Rendered right eye image
Rendered left eye image
Screen
Accommodated depth
Accommodated on the screen
Left
Accommodation matches convergence
Rendered depth
Left
Left eye
Right eye
No Focus Cues
Stereoscopic Viewing

Figure 1B

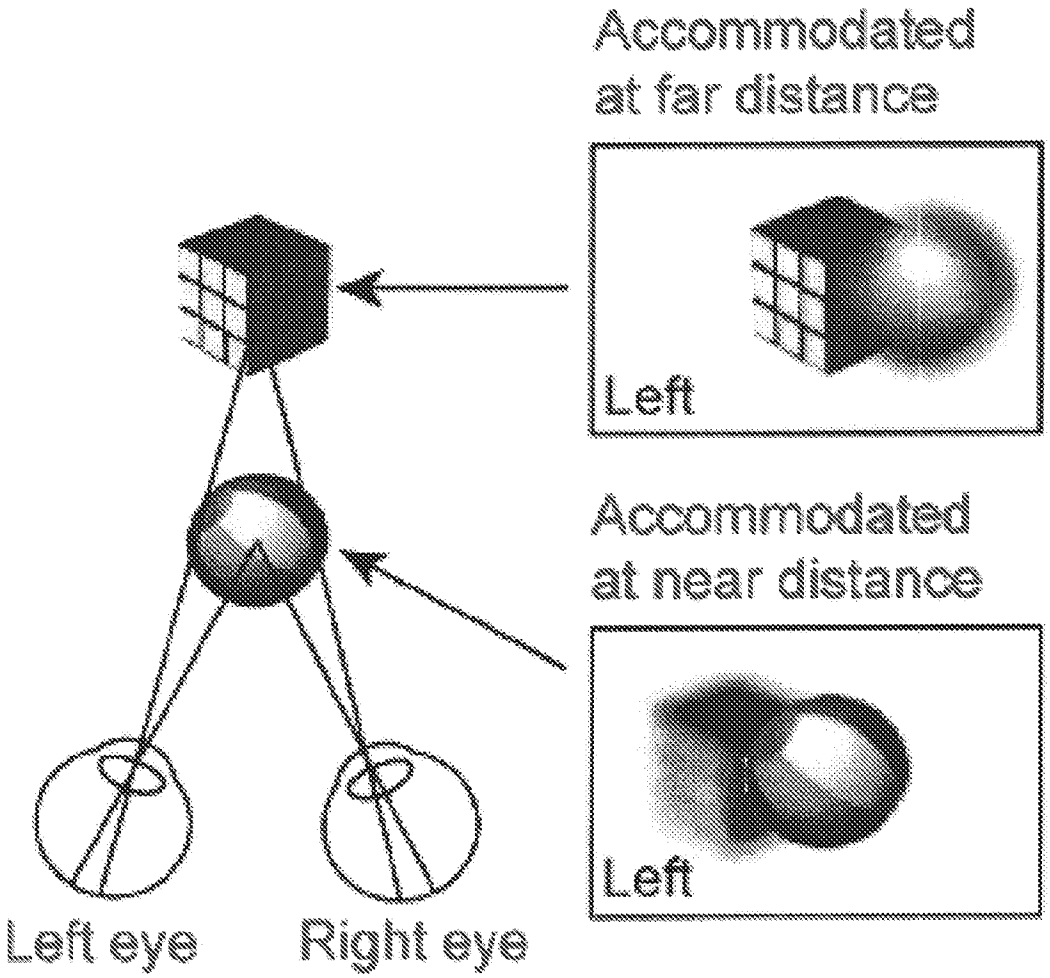
Accommodated
at far distance
Left
Accommodated
at near distance
Left
Left eye
Right eye

Figure 1C

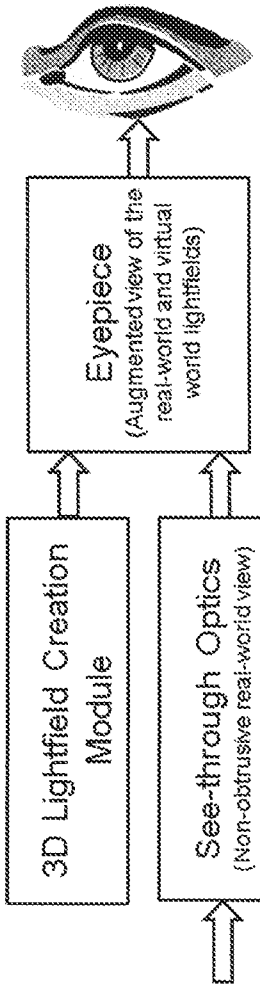
Eyepiece
(Augmented view of the real-world and virtual world lightfields)
3D Lightfield Creation Module
See-through Optics
(Non-obtrusive real-world view)

Figure 2

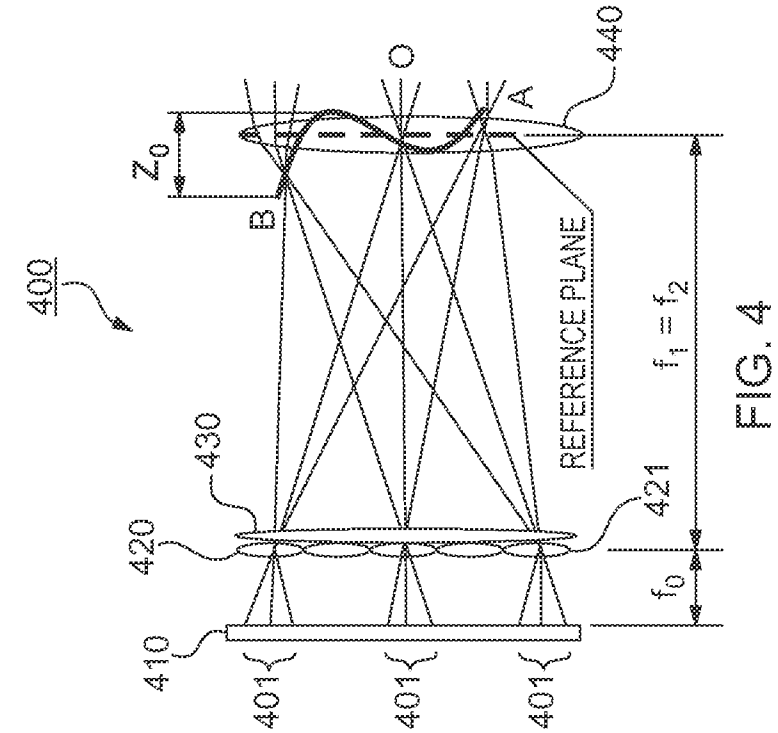
400
410
420
430
440
401
401
401
O
A
B
Z_0
REFERENCE PLANE
$f_1 = f_2$
421
f_0

FIG. 4

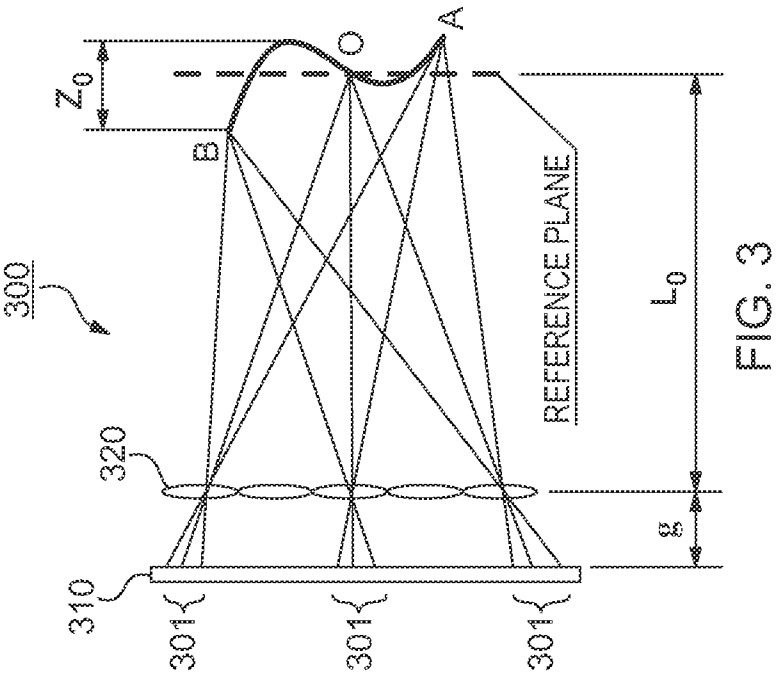
300
310
320
301
301
301
O
A
B
Z_0
REFERENCE PLANE
L_0
g

FIG. 3

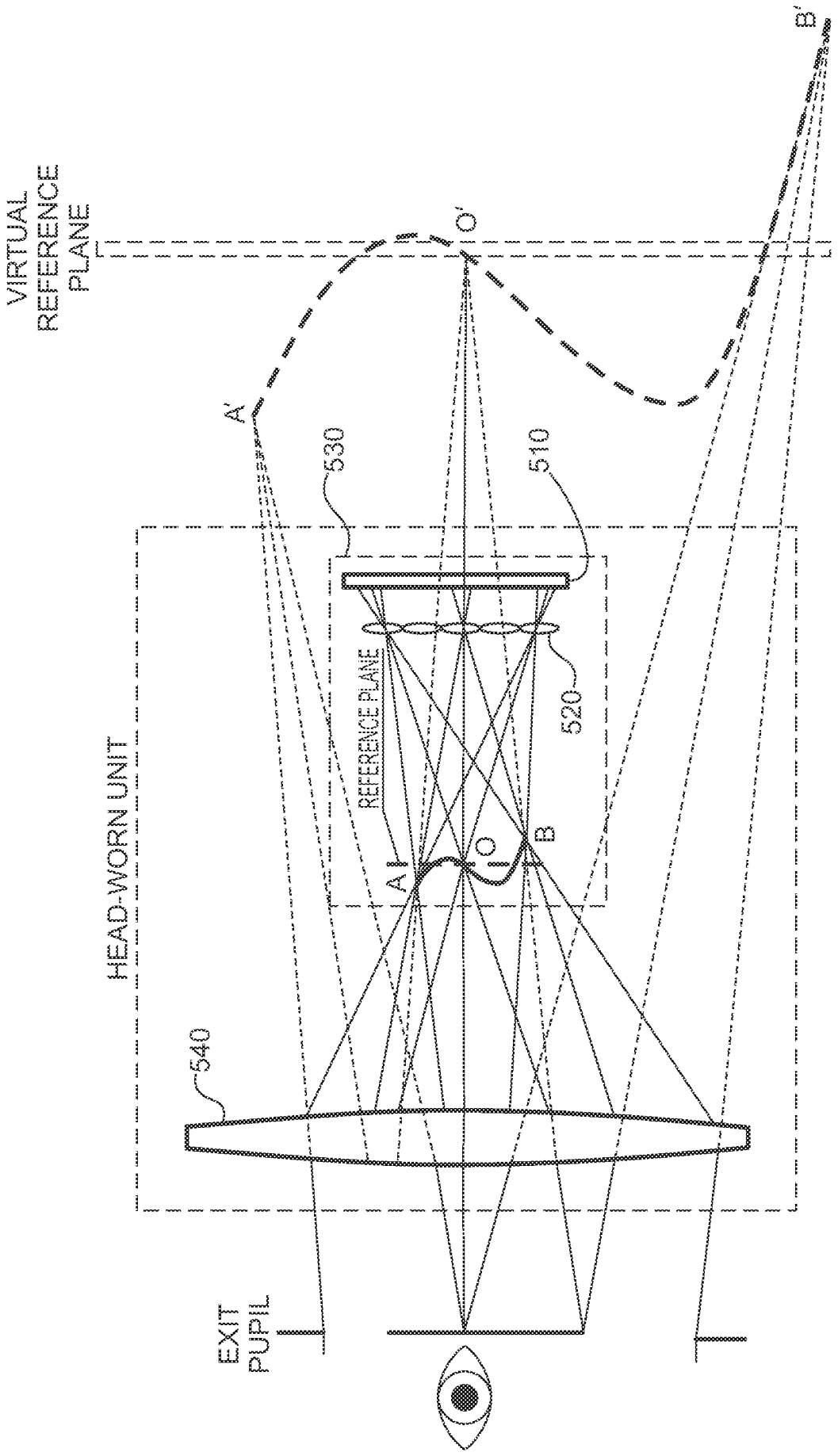
VIRTUAL REFERENCE PLANE
A'
O'
B'
530
510
520
REFERENCE PLANE
HEAD-WORN UNIT
A
O
B
540
EXIT PUPIL

FIG. 5

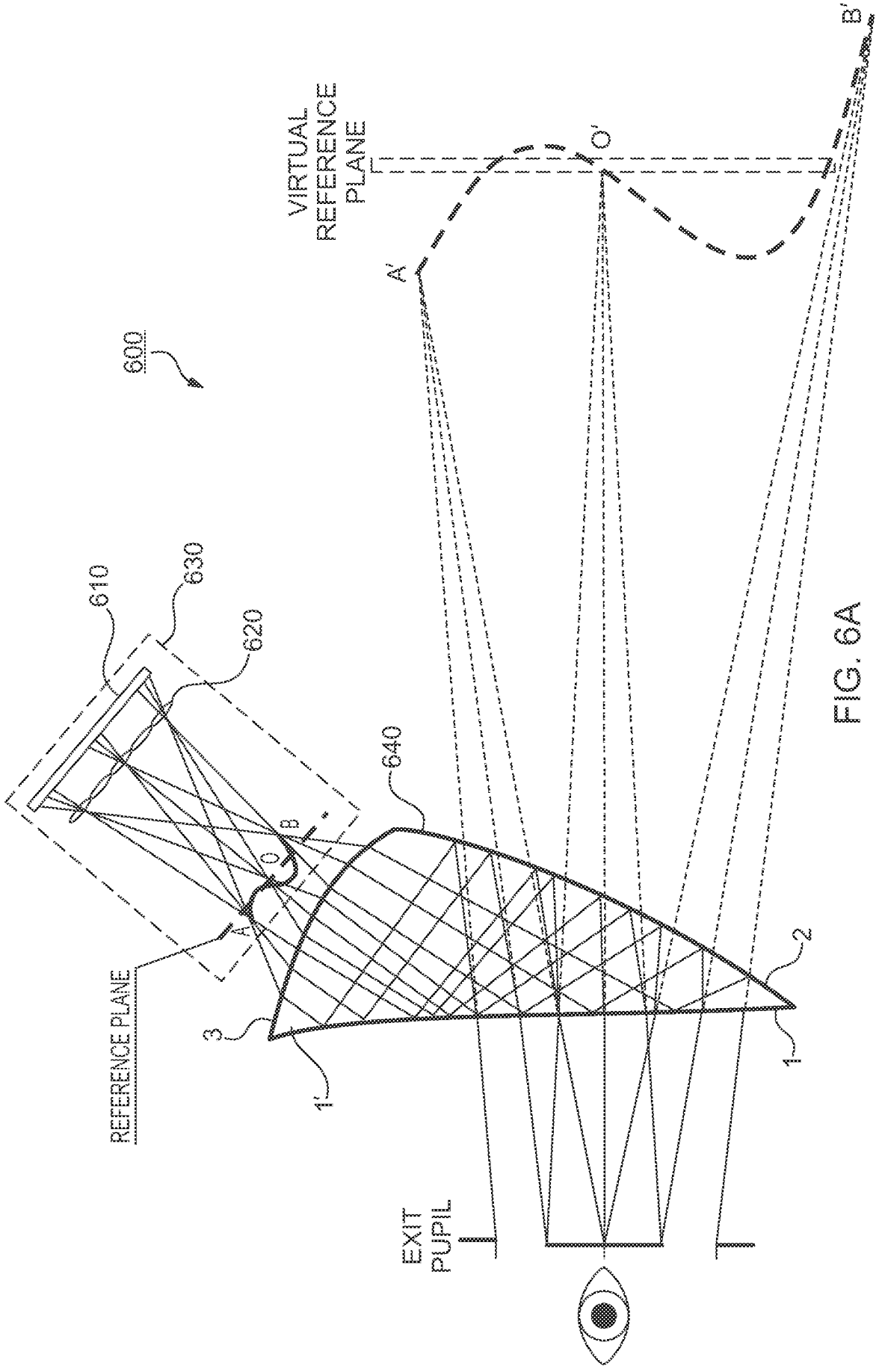
600
610
630
620
640
VIRTUAL REFERENCE PLANE
A'
O'
B'
REFERENCE PLANE
A
O
B
3
1'
1
2
EXIT PUPIL

FIG. 6A

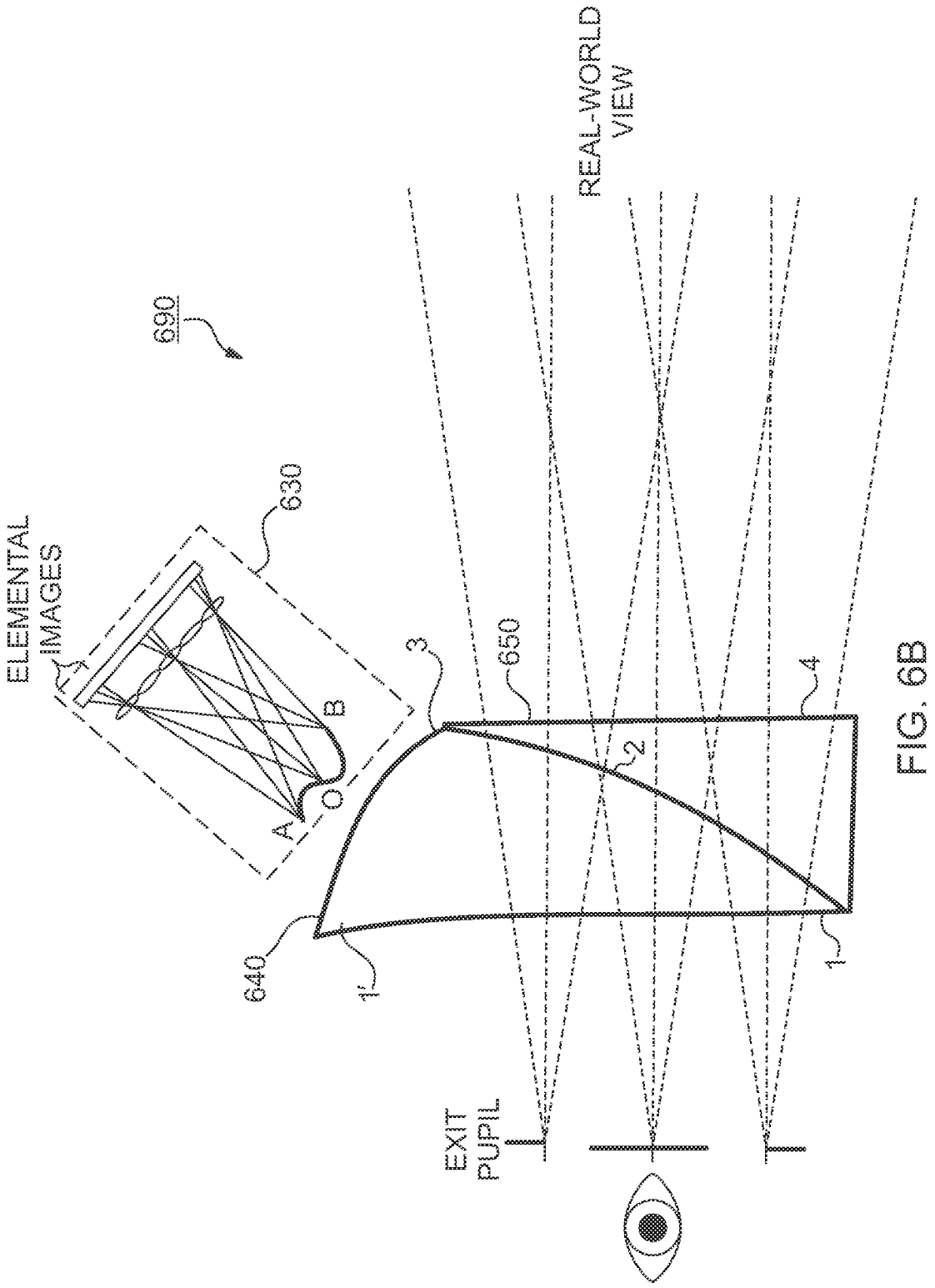
690
630
ELEMENTAL IMAGES
A
O
B
3
650
REAL-WORLD VIEW
4
2
640
1'
1
EXIT PUPIL

FIG. 6B

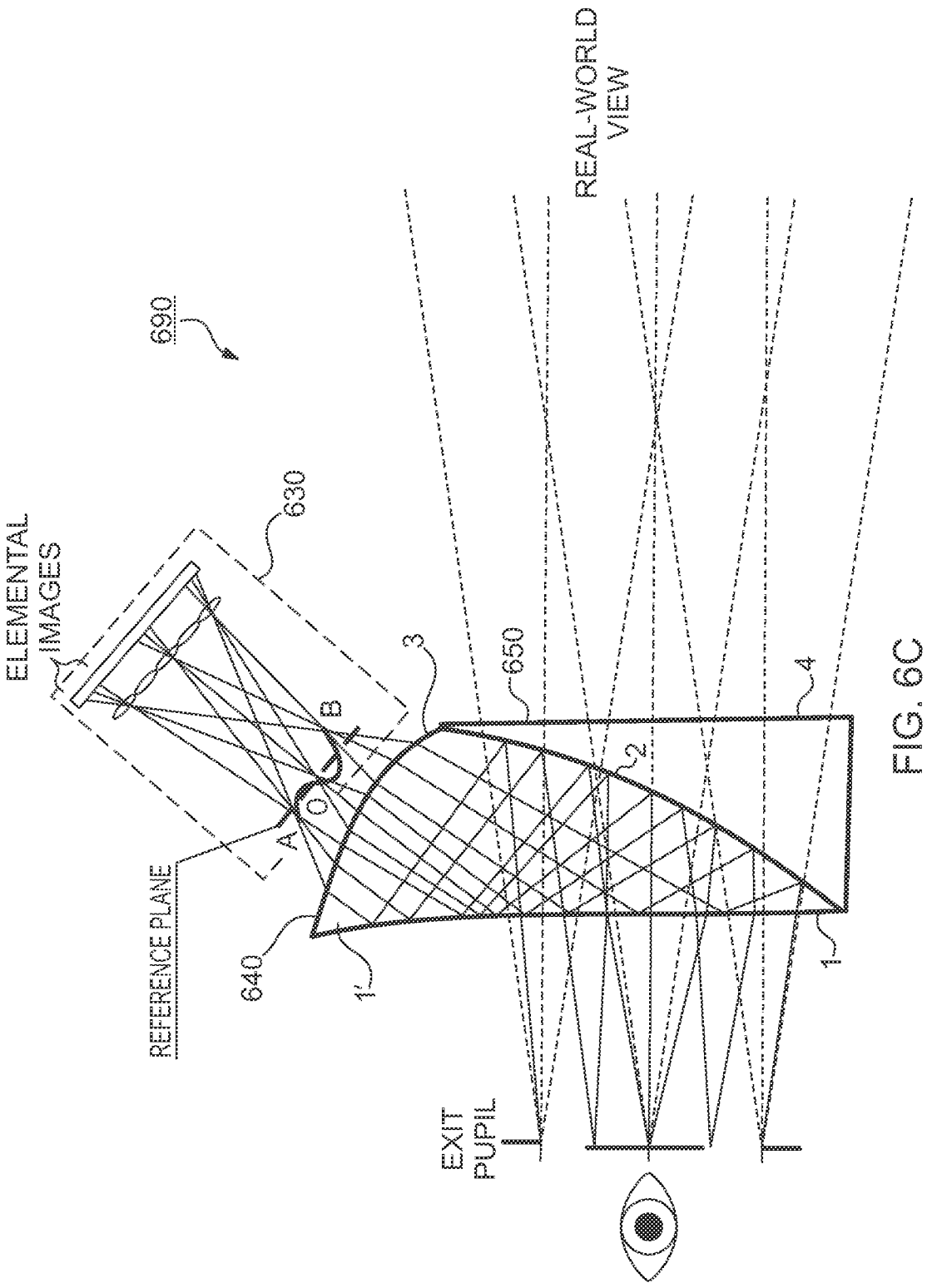
690
630
ELEMENTAL IMAGES
REAL-WORLD VIEW
650
3
4
2
1
1'
640
REFERENCE PLANE
EXIT PUPIL
A
O
B

FIG. 6C

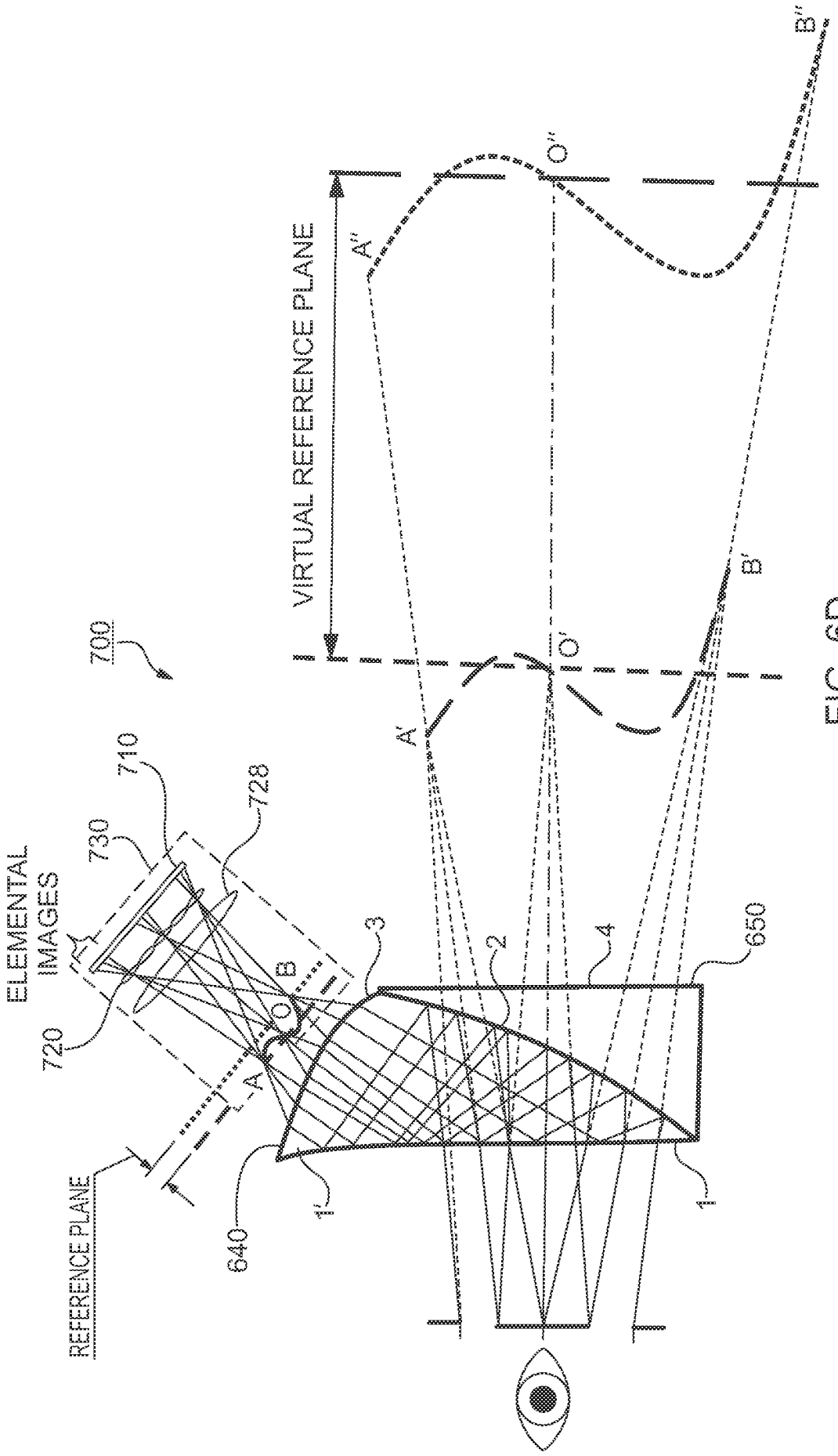
700
710
728
730
720
ELEMENTAL IMAGES
REFERENCE PLANE
640
650
VIRTUAL REFERENCE PLANE
A
B
O
A'
O'
B'
A''
O''
B''
1
2
3
4
1'

FIG. 6D

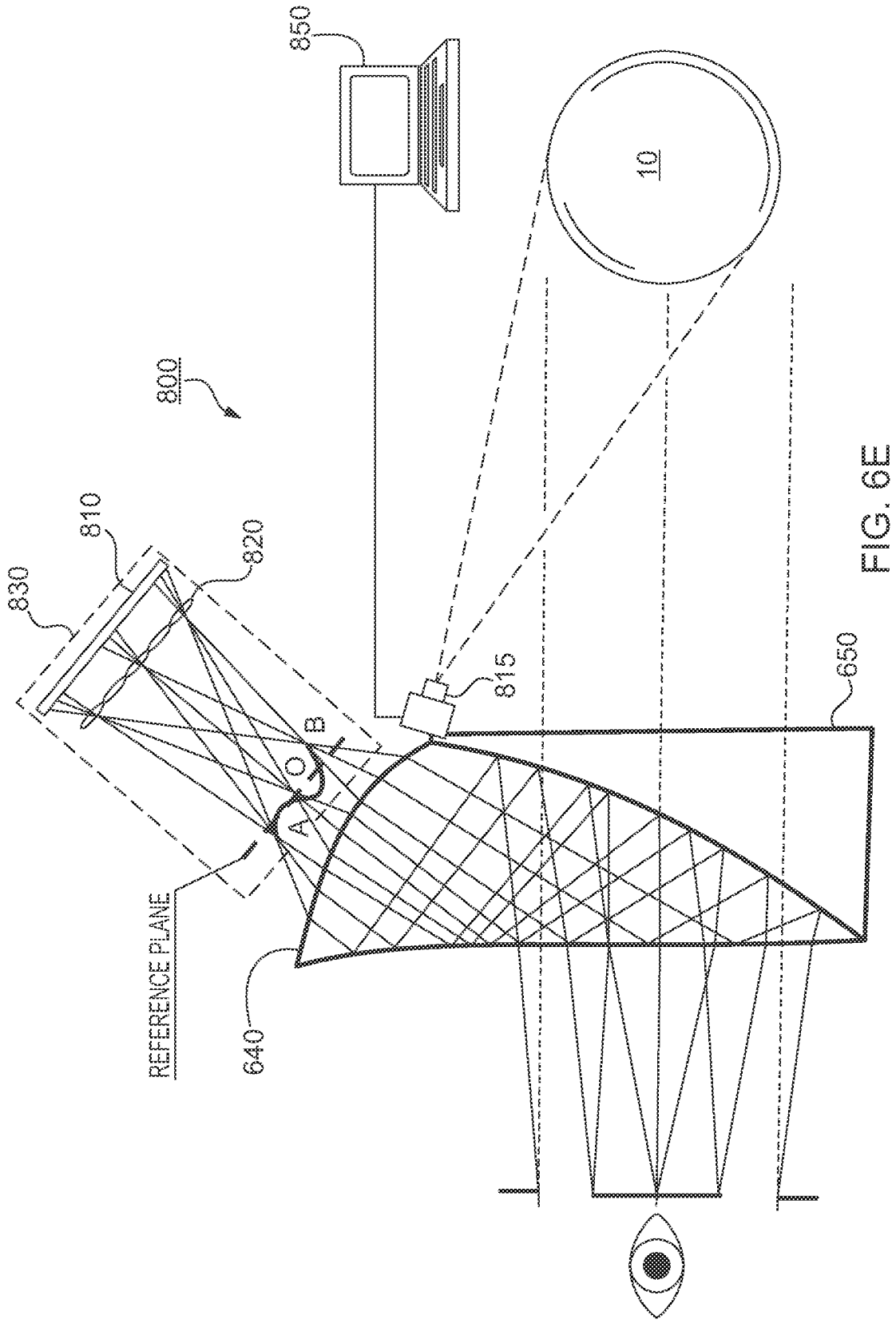

FIG. 6E

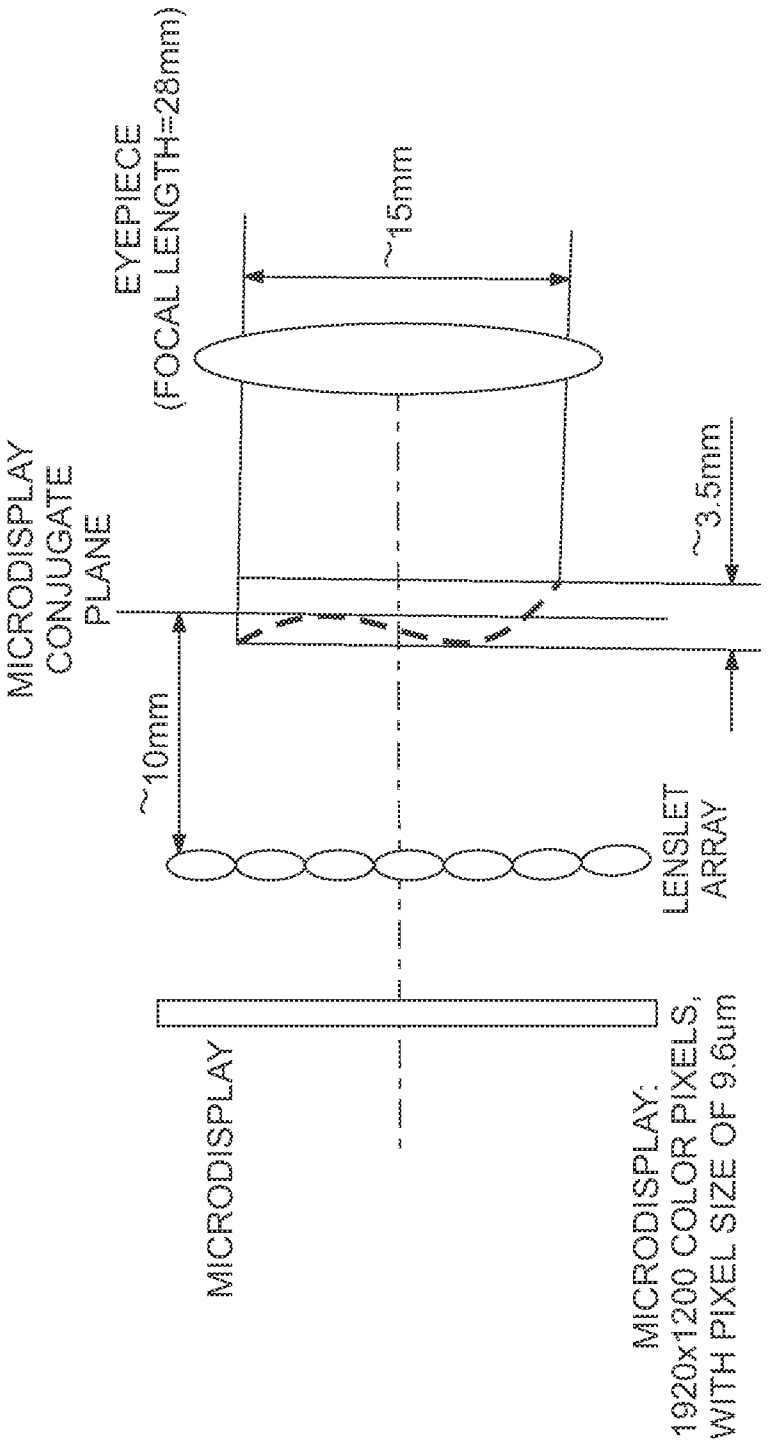
EYEPIECE
(FOCAL LENGTH=28mm)
~15mm
~3.5mm
MICRODISPLAY
CONJUGATE
PLANE
~10mm
LENSLET
ARRAY
MICRODISPLAY
MICRODISPLAY:
1920x1200 COLOR PIXELS,
WITH PIXEL SIZE OF 9.6um

FIG. 7

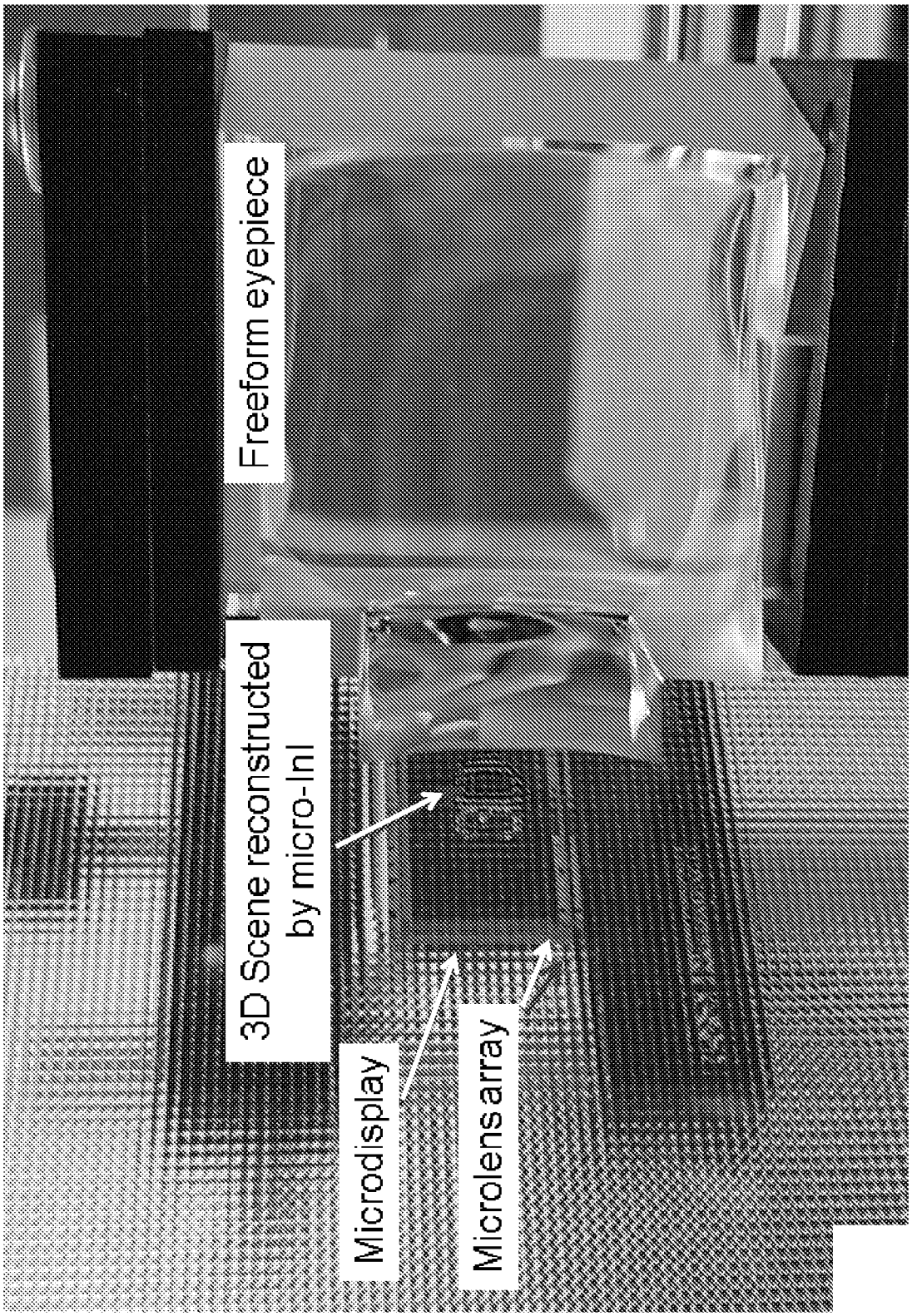
Freeform eyepiece
3D Scene reconstructed by micro-InI
Microdisplay
Microlens array

Figure 8

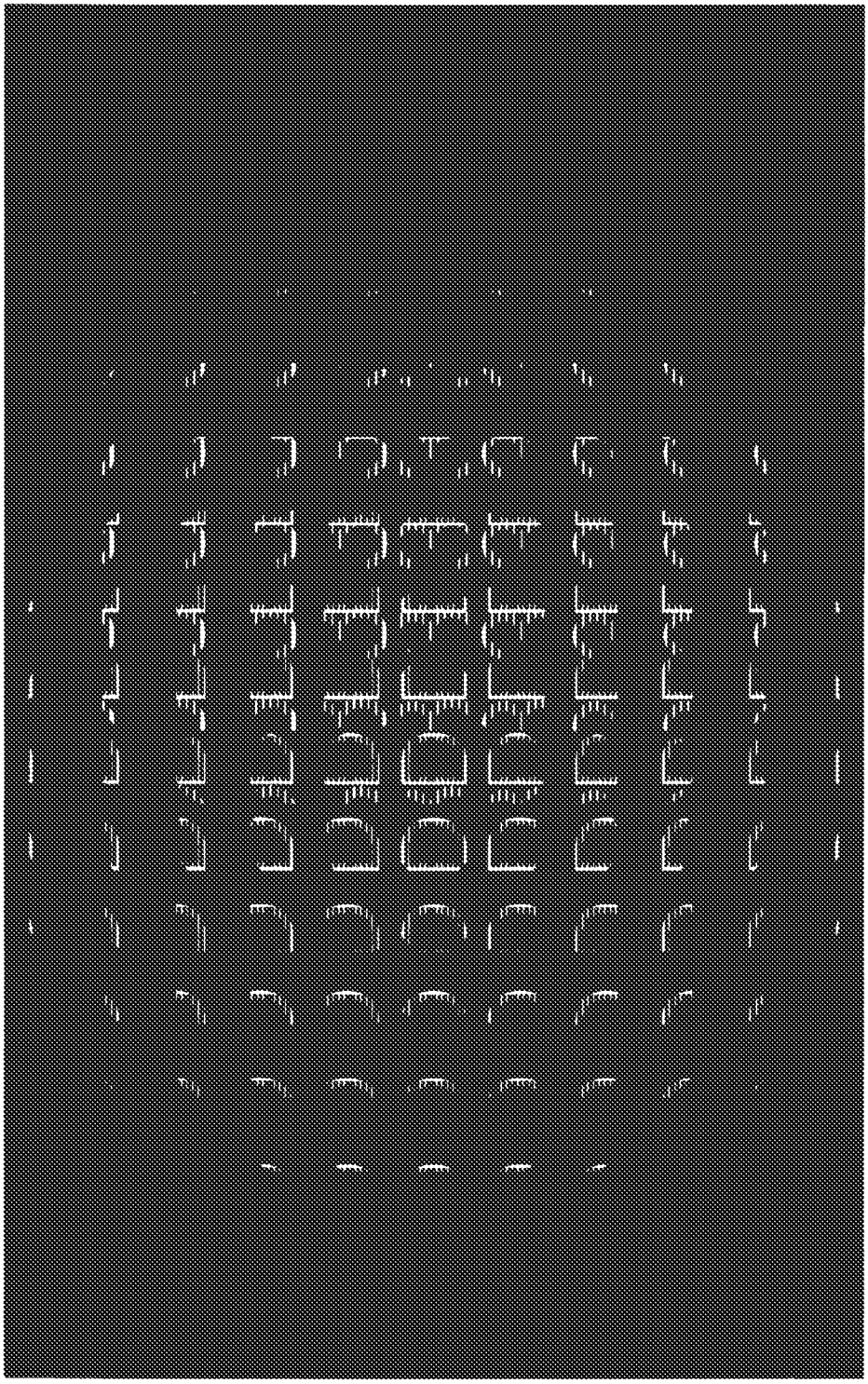

Figure 9

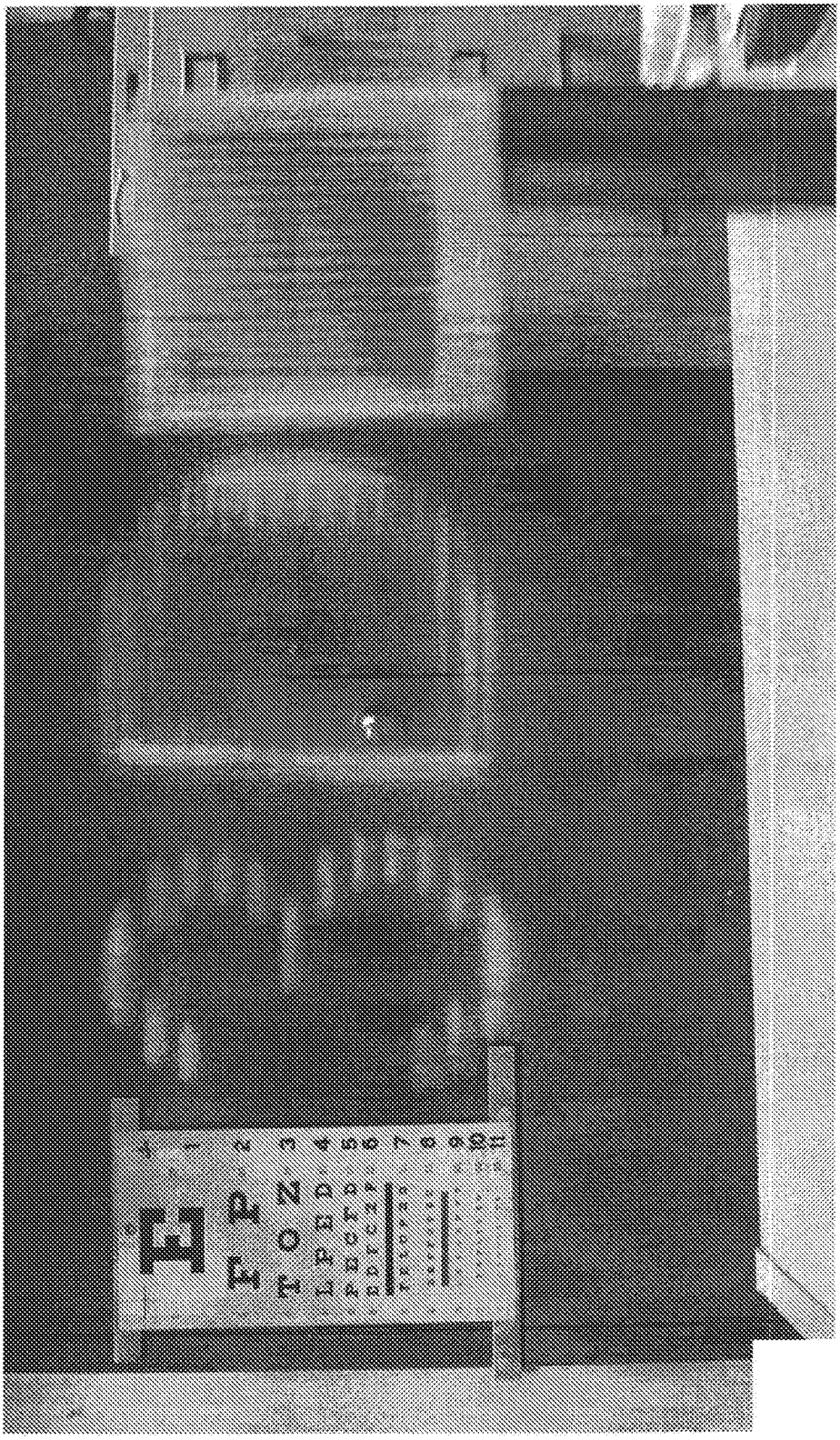

Figure 10A

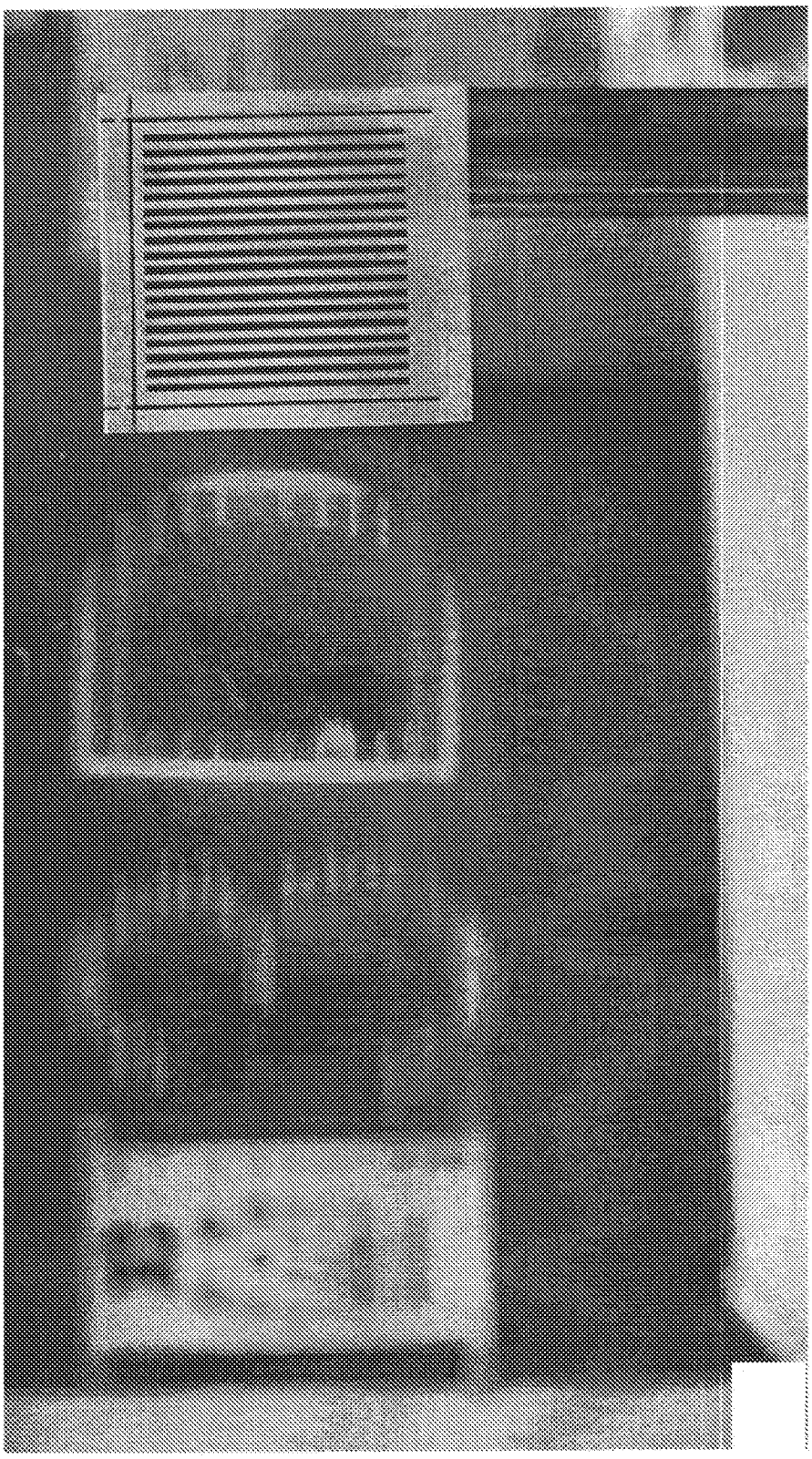

Figure 10B

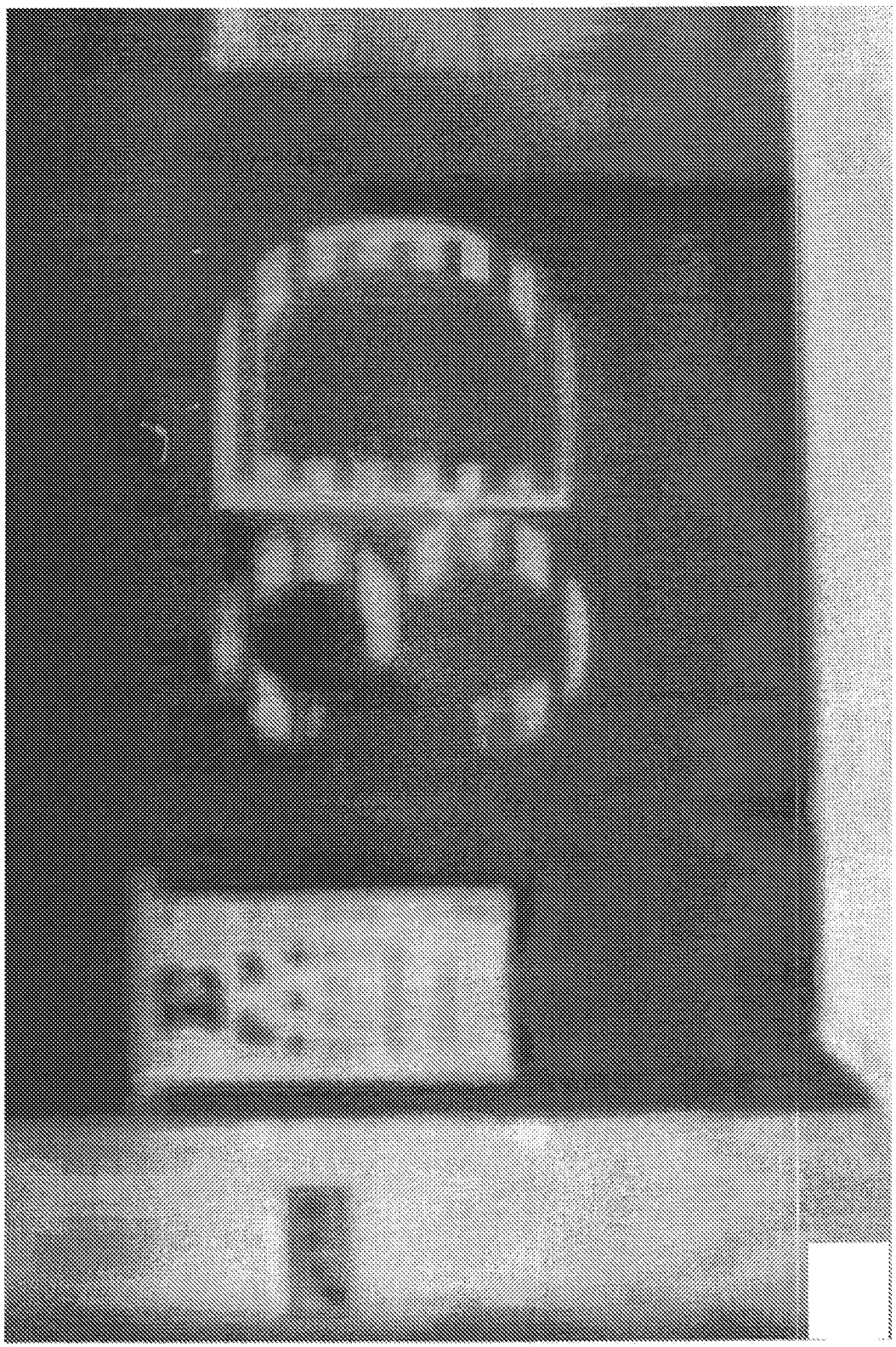

Figure 10C

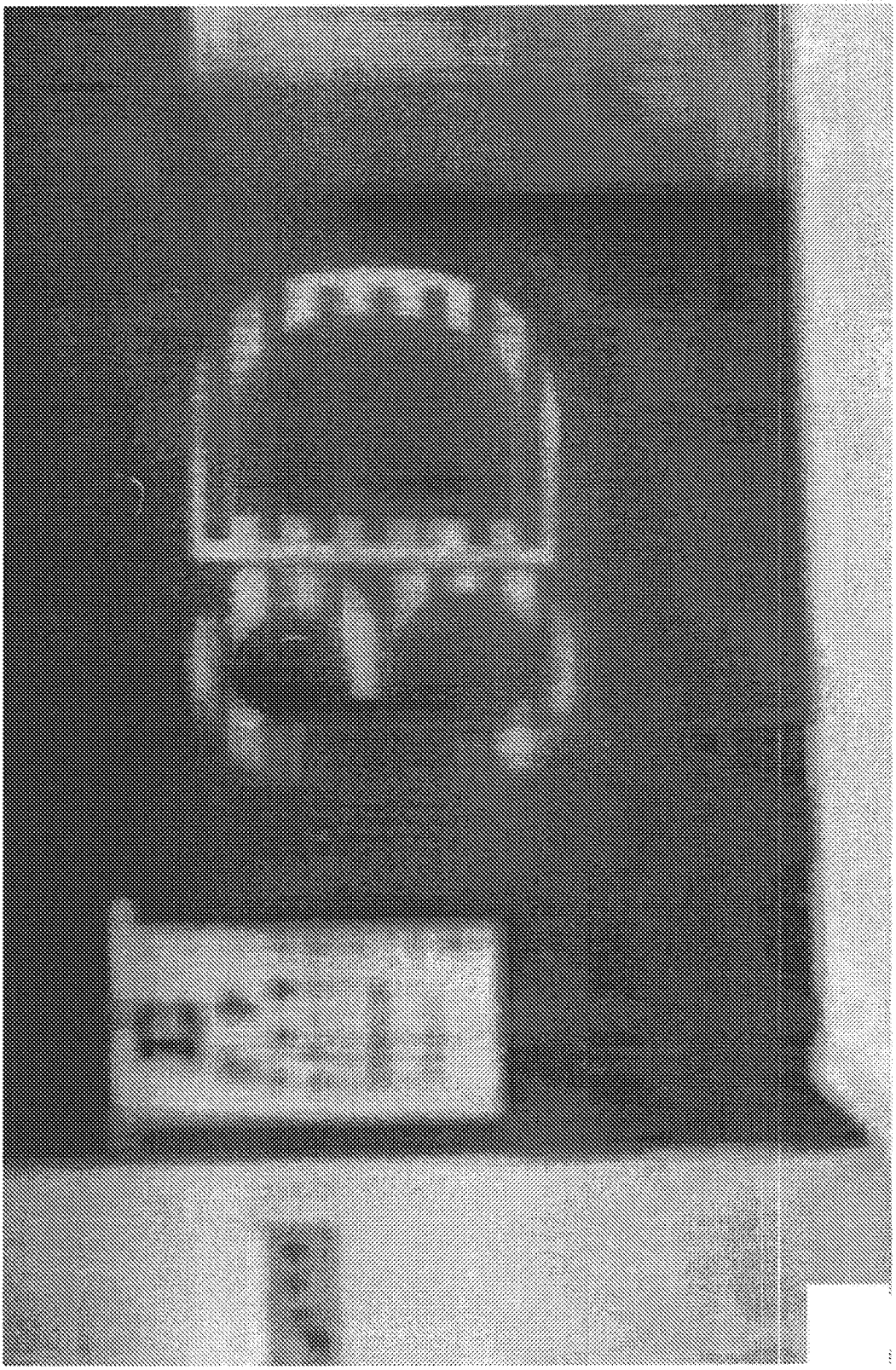

Figure 10D

INTERNATIONAL SEARCH REPORT

International application No
PCT/US2015/018951

A. CLASSIFICATION OF SUBJECT MATTER
INV. G02B27/22 G02B27/01
ADD.

According to International Patent Classification (IPC) or to both national classification and IPC

B. FIELDS SEARCHED

Minimum documentation searched (classification system followed by classification symbols)
G02B

Documentation searched other than minimum documentation to the extent that such documents are included in the fields searched

Electronic data base consulted during the international search (name of data base and, where practicable, search terms used)
EPO-Internal, WPI Data

C. DOCUMENTS CONSIDERED TO BE RELEVANT

Category*	Citation of document, with indication, where appropriate, of the relevant passages	Relevant to claim No.
X	US 2012/113092 A1 (BAR-ZEEV AVI [US] ET AL) 10 May 2012 (2012-05-10) figure 2A	1-18
X	US 2011/075257 A1 (HUA HONG [US] ET AL) 31 March 2011 (2011-03-31) figure 1	1,2
X	US 2013/300634 A1 (WHITE SEAN [US] ET AL) 14 November 2013 (2013-11-14) figures 7A-7B	1

☐ Further documents are listed in the continuation of Box C.

☒ See patent family annex.

* Special categories of cited documents :

"A" document defining the general state of the art which is not considered to be of particular relevance

"E" earlier application or patent but published on or after the international filing date

"L" document which may throw doubts on priority claim(s) or which is cited to establish the publication date of another citation or other special reason (as specified)

"O" document referring to an oral disclosure, use, exhibition or other means

"P" document published prior to the international filing date but later than the priority date claimed

"T" later document published after the international filing date or priority date and not in conflict with the application but cited to understand the principle or theory underlying the invention

"X" document of particular relevance; the claimed invention cannot be considered novel or cannot be considered to involve an inventive step when the document is taken alone

"Y" document of particular relevance; the claimed invention cannot be considered to involve an inventive step when the document is combined with one or more other such documents, such combination being obvious to a person skilled in the art

"&" document member of the same patent family

Date of the actual completion of the international search	Date of mailing of the international search report
28 May 2015	03/06/2015

Name and mailing address of the ISA/	Authorized officer
European Patent Office, P.B. 5818 Patentlaan 2 NL - 2280 HV Rijswijk Tel. (+31-70) 340-2040, Fax: (+31-70) 340-3016	Quertemont, Eric

1

INTERNATIONAL SEARCH REPORT

Information on patent family members

International application No
PCT/US2015/018951

Patent document cited in search report	Publication date	Patent family member(s)	Publication date
US 2012113092 A1	10-05-2012	AR 083807 A1	20-03-2013
		CA 2815372 A1	18-05-2012
		CN 102566049 A	11-07-2012
		EP 2638693 A1	18-09-2013
		JP 2014505381 A	27-02-2014
		KR 20130139280 A	20-12-2013
		TW 201224516 A	16-06-2012
		US 2012113092 A1	10-05-2012
		WO 2012064546 A1	18-05-2012
US 2011075257 A1	31-03-2011	NONE	
US 2013300634 A1	14-11-2013	EP 2839331 A1	25-02-2015
		US 2013300634 A1	14-11-2013
		WO 2013170073 A1	14-11-2013